Fluctuating Light Interacts with Time of Day and Leaf Development Stage to Reprogram Gene Expression[1]

Trang Schneider,[a,b,2] Anthony Bolger,[c] Jürgen Zeier,[b] Sabine Preiskowski,[a] Vladimir Benes,[d] Sandra Trenkamp,[e] Björn Usadel,[a,c] Eva M. Farré,[f] and Shizue Matsubara[a,3]

[a]IBG-2: Plant Sciences, Forschungszentrum Jülich, D-52425 Juelich, Germany
[b]Heinrich Heine University, D-40225 Duesseldorf, Germany
[c]Institute for Biology I: Institute for Botany and Molecular Genetics, RWTH Aachen University, D-52074 Aachen, Germany
[d]Genomics Core Facility, EMBL Heidelberg, D-69117 Heidelberg, Germany
[e]Metabolomic Discoveries, D-14476 Potsdam, Germany
[f]Department of Plant Biology, Michigan State University, East Lansing, Michigan 48824

ORCID IDs: 0000-0002-0272-6580 (T.S.); 0000-0002-8703-5403 (J.Z.); 0000-0002-0352-2547 (V.B.); 0000-0003-1566-7572 (E.M.F.); 0000-0002-1440-6496 (S.M.).

Natural light environments are highly variable. Flexible adjustment between light energy utilization and photoprotection is therefore of vital importance for plant performance and fitness in the field. Short-term reactions to changing light intensity are triggered inside chloroplasts and leaves within seconds to minutes, whereas long-term adjustments proceed over hours and days, integrating multiple signals. While the mechanisms of long-term acclimation to light intensity have been studied by changing constant growth light intensity during the day, responses to fluctuating growth light intensity have rarely been inspected in detail. We performed transcriptome profiling in Arabidopsis (*Arabidopsis thaliana*) leaves to investigate long-term gene expression responses to fluctuating light (FL). In particular, we examined whether responses differ between young and mature leaves or between morning and the end of the day. Our results highlight global reprogramming of gene expression under FL, including that of genes related to photoprotection, photosynthesis, and photorespiration and to pigment, prenylquinone, and vitamin metabolism. The FL-induced changes in gene expression varied between young and mature leaves at the same time point and between the same leaves in the morning and at the end of the day, indicating interactions of FL acclimation with leaf development stage and time of day. Only 46 genes were up- or down-regulated in both young and mature leaves at both time points. Combined analyses of gene coexpression and cis-elements pointed to a role of the circadian clock and light in coordinating the acclimatory responses of functionally related genes. Our results also suggest a possible cross talk between FL acclimation and systemic acquired resistance-like gene expression in young leaves.

Adjustments of photosynthetic light energy utilization and photoprotection to changing light intensity are triggered over different time scales. Rapid changes (seconds to minutes) are induced inside chloroplasts by reduction of electron transport chain or upon formation of a [H^+] gradient (ΔpH) across the thylakoid membrane. Short-term responses have been studied intensively to unveil various regulatory mechanisms involved therein. Reduction of the plastoquinone (PQ) pool by preferential excitation of PSII relative to PSI, for example, leads to activation of thylakoid protein kinase STN7, which phosphorylates PSII light-harvesting complex (LHC) to trigger its displacement from PSII to PSI in a process termed state transition (Bellafiore et al., 2005). Light-dependent acidification of thylakoid lumen protonates the PSBS protein to quickly induce thermal energy dissipation (or nonphotochemical quenching [NPQ]) and thus down-regulate PSII (Li et al., 2000). Lumen acidification also activates a xanthophyll-cycle enzyme, violaxanthin deepoxidase (VDE), to convert violaxanthin to antheraxanthin and zeaxanthin, which enhances NPQ (Niyogi et al., 1998). Furthermore, alternative electron (e^-) flows (e.g. water-water cycle and cyclic e^- flow [CEF] around PSI), by which electrons are transferred from PSI to water through Mehler-ascorbate peroxidase reactions (Asada, 1999) or

[1]This work was supported by Deutsche Forschungsgemeinschaft (IRTG 1525).

[2]Present address: KWS LOCHOW GmbH, D-29303 Bergen, Germany.

[3]Author for contact: s.matsubara@fz-juelich.de.

The author responsible for distribution of materials integral to the findings presented in this article in accordance with the policy described in the Instructions for Authors (www.plantphysiol.org) is: Shizue Matsubara (s.matsubara@fz-juelich.de).

T.S. and S.M. designed the experiments; T.S. performed most of the experiments and data analyses; A.B. and T.S. analyzed the RNA-Seq data; V.B. and S.T. provided technical assistance for the RNA-Seq and metabolome analyses; J.Z. did gene expression comparison of highly upregulated genes; S.P. performed part of the RT-qPCR experiments; E.M.F., J.Z., B.U., and S.M. supervised the experiments and data analyses; S.M. conceived the project and wrote the article with contributions from T.S., E.M.F., and J.Z.

www.plantphysiol.org/cgi/doi/10.1104/pp.18.01443

from ferredoxin (FD) back to PQ (Johnson, 2011; Yamori and Shikanai, 2016), can support ΔpH formation and hence ATP synthesis and NPQ. In the chloroplast stroma, the thioredoxin (TRX) system mediates light- and redox-dependent regulation of enzyme activities, including those in the Calvin-Benson cycle (CBC) and oxidative pentose phosphate pathway or ATP and starch synthesis (Schürmann and Buchanan, 2008).

Long-term changes in growth light environment, on the other hand, elicit acclimatory responses that are slowly inducible and reversible (hours to days) or irreversible. Inside chloroplasts, the relative abundance of photosynthetic protein complexes changes in response to prevailing growth light intensity. High-light (HL) and sunlit conditions favor accumulation of PSII, cytochrome b_6f (Cyt b_6f), and ATP synthase but suppress LHCII (major LHC of PSII) compared with low-light (LL) and shaded conditions (Evans, 1987; Anderson et al., 1988). In addition, HL and excess light (EL) increase leaf carotenoid content, especially the xanthophyll cycle components, along with other antioxidants like tocopherols, ascorbate, and glutathione (Demmig-Adams and Adams, 1992; Grace and Logan, 1996; Bartoli et al., 2006; Lichtenthaler, 2007; Matsubara et al., 2009). Together, these biochemical modifications contribute to enhancement of photosynthetic e^- transport, CO_2 assimilation, NPQ, and reactive oxygen species (ROS) scavenging in HL and EL.

Unlike locally controlled short-term responses, long-term acclimation can be observed in both local and distant tissues. Elongation growth of palisade cells is locally controlled via UV-A and blue light photoreceptor phototropins (Kozuka et al., 2011), which also regulate short-term responses of chloroplast movement and stomatal opening (Christie et al., 2018). In contrast, formation of extra palisade cell layers has been seen in leaf primordia and young growing leaves when mature leaves are exposed to HL (Terashima et al., 2006). Changes in these anatomical traits result in leaf thickening and enlargement of palisade cell surface area to facilitate chloroplast CO_2 uptake in HL (Terashima et al., 2006). Additionally, thick leaves can accumulate more photosynthetic enzymes per unit of leaf area, which also contributes to greater CO_2 fixation capacity of HL-grown leaves per unit of leaf area (but not necessarily per unit of leaf mass; Givnish, 1988; Evans and Poorter, 2001). As for photoprotection, systemic acquired acclimation has been reported in young leaves when mature leaves are exposed to EL and HL (Karpinski et al., 1999). Since light and carbon are not limiting for plant growth in HL, whole-plant biomass allocation shifts toward roots to ensure water and nutrient uptake (Poorter et al., 2012).

Fluctuating growth light environments induce long-term acclimatory responses that are distinct from those found in LL or HL. Acclimatory responses to fluctuating light (FL) are influenced by duration, frequency, and amplitude of fluctuations. When LL-grown (100 μmol photons m^{-2} s^{-1}) plants of Arabidopsis (*Arabidopsis thaliana*) were transferred to conditions in which light intensity was fluctuating between 100 and 475 or between 100 and 810 μmol photons m^{-2} s^{-1} every 15 min, 1 h, or 3 h during the daytime, oxygen evolution capacity of PSII increased in all FL conditions compared with LL (Yin and Johnson, 2000). Yet, the efficacy to induce this up-regulation varied in different FL conditions; a 3-h cycle was the most effective regime in 100/475 μmol photons m^{-2} s^{-1}, whereas a 15-min cycle allowed the largest increase in oxygen evolution under 100/810 μmol photons m^{-2} s^{-1} (Yin and Johnson, 2000). In marked contrast, Arabidopsis plants grown under FL, which consisted of short (20-s) pulses of HL (650 or 1,250 μmol photons m^{-2} s^{-1}) applied every 6 or 12 min under LL (50 μmol photons m^{-2} s^{-1}), up-regulated the capacities for NPQ and ROS scavenging while reducing the PSII efficiency, chlorophyll (Chl) and carbohydrate contents, as well as leaf growth (Alter et al., 2012). In conditions mimicking natural light fluctuations, Arabidopsis leaves became thinner than in fixed intensity (constant light [CL]) of the same average intensity and daylength while maintaining similar CO_2 fixation rates per unit of leaf area (Vialet-Chabrand et al., 2017). Generally, however, responses to FL (and also HL and LL) are dependent on species, preexperimental conditions, and other environmental, physiological, and developmental factors (Chazdon and Pearcy, 1986; Tinoco-Ojanguren and Pearcy, 1992; Watling et al., 1997a, 1997b; Yin and Johnson, 2000; Leakey et al., 2003; Kaiser et al., 2018a).

Unraveling molecular mechanisms (or networks) of long-term acclimation is hampered by the complexity arising from a mixture of interlinked or unrelated reactions that are induced concurrently or sequentially over time. Nonetheless, studies in the past ~20 years have led to identification of signaling agents and pathway components involved in acclimation to growth light environments, including EL and photooxidative stress. Energy transfer from Chl to oxygen generates singlet oxygen ($^1O_2$) especially in PSII. The core complexes of PSII and PSI bind β-carotene molecules that can be oxidized by (and thereby detoxify) $^1O_2$. It has been proposed that some apocarotenoids, which are derived from oxidative cleavage of β-carotene, may serve as stress signals to elicit EL acclimation; when applied to nonstressed leaves of Arabidopsis, an apocarotenoid volatile (β-cyclocitral) was able to induce the expression of $^1O_2$-responsive genes (Ramel et al., 2012; Havaux, 2014). Another stress signal originates from the plastidic methylerythritol phosphate (MEP) pathway, which synthesizes isoprenoid precursors; a MEP pathway intermediate, 2-*C*-methyl-D-erythritol-2,4-cyclodiphosphate (MEcPP), is able to activate the transcription of stress-responsive genes, such as *ISOCHORISMATE SYNTHASE1* (*ICS1*), alias *SALICYLIC ACID INDUCTION DEFICIENT2*, which encodes an enzyme in salicylic acid (SA) biosynthesis (Xiao et al., 2012; de Souza et al., 2017). Under HL or drought stress, leaves accumulate 3′-phosphoadenosine 5′-phosphate, a by-product of sulfotransferase reactions

to make sulfated compounds; it is thought that 3′-phosphoadenosine 5′-phosphate inhibits 5′-3′ exoribonuclease activity to modulate HL- and oxidative stress-related gene expression (Estavillo et al., 2011; Chan et al., 2016).

The molecular mechanisms of long-term acclimation to growth light intensity have been studied by transferring plants from constant LL to constant HL (or EL) and vice versa. Long-term acclimation to fluctuating growth light intensity has rarely been investigated, even though FL constitutes a substantial part of daily light exposure for inner-canopy leaves and understory plants (Pearcy, 1990; Kaiser et al., 2018b; Slattery et al., 2018). Sunlight intensity fluctuates also for outer-canopy leaves as clouds travel and the weather changes. Long-term mechanisms of FL acclimation are therefore of great relevance to understanding how plants respond to growth light conditions in the field. Here, we conducted transcriptome profiling in Arabidopsis leaves, focusing on long-term acclimation to the FL conditions that primarily elicit EL and photooxidative stress responses (Alter et al., 2012). In particular, we asked whether acclimatory adjustment of gene expression varies between growing (Young) and non-growing (Mature) leaves because stress signaling and acclimation (biochemical, morphological, or developmental) may differ between these leaves (Chan et al., 2016). Given the pronounced diurnal variations in gene expression in leaves (Bläsing et al., 2005; Michael et al., 2008b), we also investigated time of day-dependent gene expression responses to FL by analyzing leaf transcriptome in the morning (MO; 1 h after the light was turned on) and at the end of the day (EOD; 1 h before the light was turned off). The results highlight global reprogramming of gene expression during long-term acclimation to FL and indicate strong interactions with both leaf development stage and time of day. The acclimatory responses of functionally related genes seem to be coordinated by the circadian clock and light signaling in leaves. Our data also suggest a possible cross talk between FL acclimation and systemic acquired resistance (SAR)-like gene expression in Young leaves.

RESULTS

The FL Treatment Induced Photooxidative Stress Responses

After germination and cultivation in a CL condition (75 μmol photons m^{-2} s^{-1} during the light period of 12 h/12 h light/dark) for approximately 4 weeks, half of the plants (Columbia-0 [Col-0]) were transferred to a corner of the same climate chamber where the automatically moving light-emitting diode (LED) device (Alter et al., 2012) was creating light fluctuations between 75 (the CL background; ~280 s) and 1,000 μmol photons m^{-2} s^{-1} (~20 s) during the light period. The other half was kept under CL. Based on our previous studies, which had shown acclimatory enhancement of photoprotective capacities in Arabidopsis following 3-d exposure to similar FL conditions (Alter et al., 2012; Caliandro et al., 2013), we took leaf samples for RNA sequencing (RNA-Seq) after 3 d under FL or CL.

To directly compare gene expression and phenotypic changes, we characterized physiological and metabolic alterations in leaves during the FL treatment. The plants were visually indistinguishable after growing under FL or CL for 3 d (Fig. 1A). Figure 1B shows Young and Mature leaves used for different analyses. Although there was no visible sign of stress on day 3, the maximal PSII efficiency (F_v/F_m) was slightly reduced in both Young and Mature leaves under FL compared with CL (Fig. 2A). As in the previous studies (Alter et al., 2012; Caliandro et al., 2013), rapid light-response curves of relative electron transport rate (ETR), which were measured in dark-adapted plants during exposure to stepwise increases in light intensity (20 s at each light level) on day 3, confirmed lower PSII activity and increased NPQ capacity in the FL plants (Fig. 2, B and C). When the leaves were allowed to reach steady state in saturating light intensity (800 μmol photons m^{-2} s^{-1}), however, the J_{max} and V_{cmax} obtained from CO_2 response curves (A/C_i curves; 4–5 min at each CO_2 level) indicated no change in the capacities for ribulose-1,5-bisphosphate (RuBP) regeneration and Rubisco carboxylation in Mature leaves after 3 d under FL (Fig. 2D). Nevertheless, leaf growth suppression in the FL condition became gradually evident between day 3 and day 7 (Fig. 2E). The plants under the FL condition had 16% less rosette dry weight than those under the CL condition on day 7 (Fig. 2F) due to reduced leaf expansion (Fig. 2E) and dry mass accumulation per unit of leaf area (Fig. 2G).

Consistent with the growth reduction under FL, the levels of Suc and starch (Fig. 3, A and B) and all free

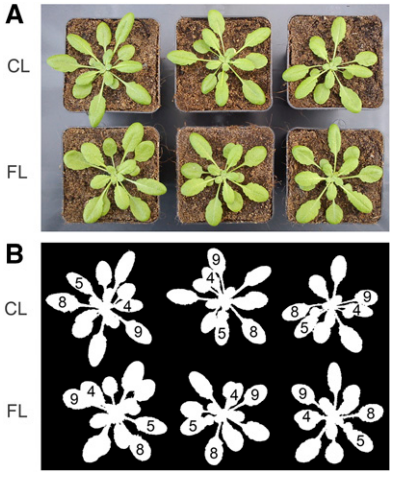

Figure 1. Arabidopsis plants after 3-d exposure to the FL or CL condition. A, Color image of CL (top row) and FL (bottom row) plants. B, The corresponding mask image showing Young (leaf 4 and 5) and Mature (leaf 8 and 9) leaves.

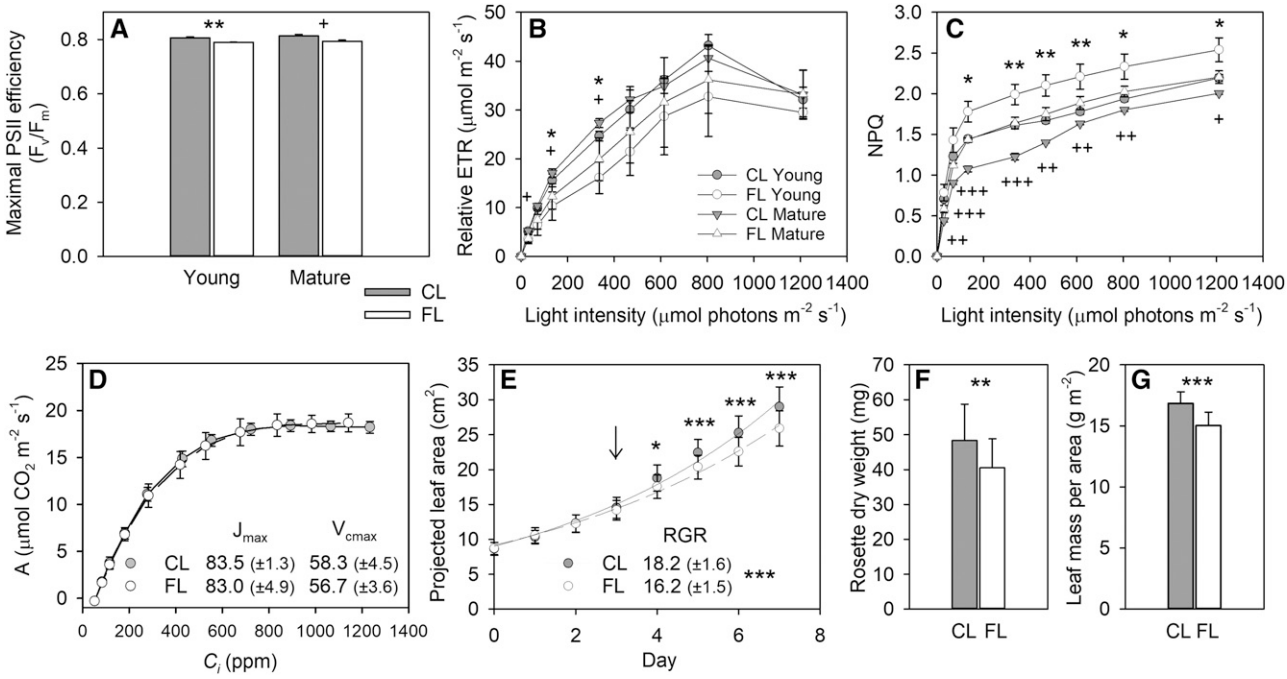

Figure 2. Changes in PSII activity, CO_2 assimilation, and leaf growth. A to C, The F_v/F_m (A), rapid light response curves of relative ETR (B), and NPQ (C) were measured in Young and Mature leaves after 3-d exposure to FL or CL. Data are means ± SD, $n = 3$. D, A/C_i curves measured in Mature leaves after 3-d exposure to FL or CL. Data were recorded at steady state in saturating light intensity (800 μmol photons m^{-2} s^{-1}). The maximum rates of RuBP regeneration (J_{max}; μmol m^{-2} s^{-1}, ±SD) and Rubisco carboxylation (V_{cmax}; μmol m^{-2} s^{-1}, ±SD) were calculated by fitting the A/C_i curves according to Sharkey et al. (2007). Data are means ± SD, $n = 5$. E, Increase in projected leaf area during the 7-d experiment. Data are means ± SD, $n = 45$ and 42 for FL and CL, respectively. The relative growth rate (RGR; % d^{-1}, ±SD) was calculated by fitting the leaf area data to an exponential growth function (R^2 = 0.9913 and 0.9885 for FL and CL, respectively). Leaf samples were taken on day 3 (arrow) for different analyses. For metabolome analysis, Mature leaves were collected on day 7. F and G, The dry weight of rosette (F) and leaf dry mass per area (G) at the end of the 7-d treatment. Data are means ± SD, $n = 17$ and 20 for FL and CL, respectively. Asterisks and plus signs in A to C denote significant differences between FL and CL for Young and Mature leaves, respectively (*** and $^{+++}$, $P < 0.001$; ** and $^{++}$, $P < 0.01$; * and $^{+}$, $P < 0.05$ by Student's t test). Asterisks in E to G are for significant differences between the plants grown under FL and CL.

amino acids except Glu and Asn at EOD (Supplemental Fig. S1) tended to decline in leaves on day 3. While FL did not affect Chl content by day 3 (Fig. 3C), it enhanced carotenoid accumulation (Fig. 3D), especially the xanthophyll cycle pigments (Fig. 3E). These phenotypic changes (Figs. 2 and 3) confirm our previous finding that short HL pulses of FL, regardless of whether they increase the average light intensity compared with CL, do not promote growth but trigger EL and photooxidative stress responses in LL-grown Arabidopsis (Alter et al., 2012).

Long-term effects of FL on the metabolome were also analyzed in Mature leaves on day 7 (Supplemental Table S1). The results corroborated the reduced accumulation of sugars and amino acids under FL especially in MO, while the levels of other metabolites (e.g. mannitol-1-phosphate, glycerate, phytol, ketolutein, ginkgolide, and theophylline) significantly increased. Arbutin, a glycosylated hydroquinone that interacts with membrane lipids and acts as an antioxidant, also showed an increase. At EOD, the leaves under FL had larger amounts of organic acids and glycerolipids with polyunsaturated fatty acids (18:3) than those under CL. Another striking change under FL was the enhanced accumulation of vitamin C-related compounds (ascorbate, dehydroascorbate, threonate, gulonate, and ketogulonolactone). Collectively, the metabolic alterations under FL can be summarized as increased antioxidant and lipid metabolism with less accumulation of sugars, starch, and amino acids, providing further support to the above-described photoprotective and photooxidative stress responses and growth inhibition.

Leaf Transcriptome Profiles of Long-Term FL Acclimation

Changes in gene expression were studied in Young and Mature leaves harvested in MO and at EOD of day 3 (hereafter Young-MO, Young-EOD, Mature-MO, and Mature-EOD). The RNA-Seq data were filtered by counts per million (CPM > 3) and false discovery rate (FDR < 0.01). Nearly all genes that satisfied these criteria showed greater than ±30% changes in expression under FL (FL/CL ≥ 1.3 or ≤ 0.7; Supplemental Fig. S2).

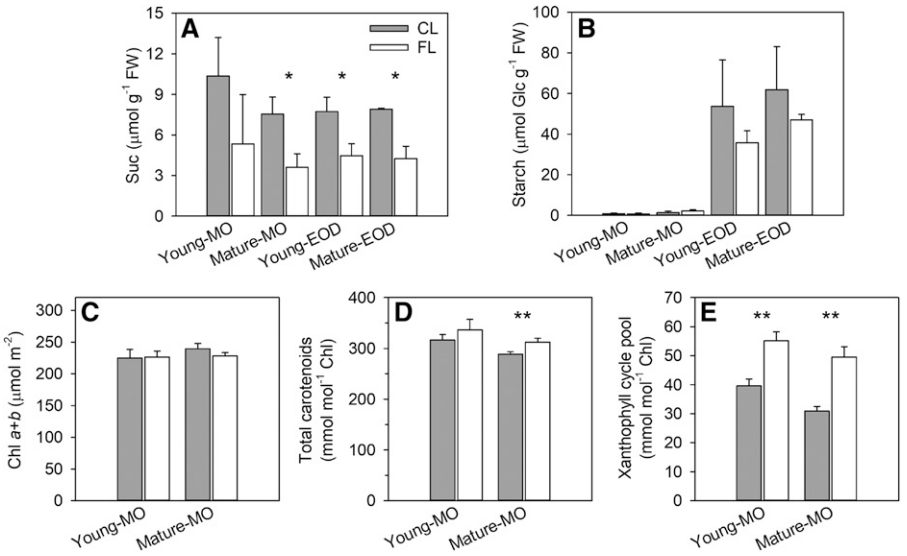

Figure 3. Nonstructural carbohydrate and photosynthetic pigment contents of Young and Mature leaves on day 3. A and B, Levels of Suc (A) and starch (B; determined as Glc) in MO and at EOD. Data are means ± SD, $n = 3$. FW, Fresh weight. C to E, Levels of Chls (C), carotenoids (D), and xanthophyll cycle pigments (E) in MO. Data are means ± SD, $n = 4$. Asterisks denote significant differences between FL and CL (**, $P < 0.01$ and *, $P < 0.05$ by Student's t test).

Since our FL treatment did not induce severe stress symptoms, we set the threshold at ±30% to take into account strongly expressed genes (e.g. photosynthetic genes) that may not undergo large relative variations.

The results of RNA-Seq analysis were validated by reverse transcription quantitative PCR (RT-qPCR) in the same samples. Four genes were selected to cover a wide range of fold change: *LHCB1.2* (*PSII LIGHT HARVESTING COMPLEX1.2*), *GPX7* (*GLUTATHIONE PEROXIDASE7*), *ELIP2* (*EARLY LIGHT-INDUCED PROTEIN2*), and *PR2* (*PATHOGENESIS-RELATED2*). The RT-qPCR data quantitatively confirmed the fold change values of RNA-Seq (Supplemental Fig. S3), with a single outlier (*ELIP2* in Mature-EOD) for which RNA-Seq gave a higher value.

Figure 4 illustrates the numbers of differentially expressed (DE) genes under FL compared with CL. More genes were up-regulated than down-regulated after a 3-d FL exposure (Fig. 4A). Many DE genes were shared by Young and Mature leaves in MO, whereas their gene expression responses to FL differed remarkably at EOD (Fig. 4B). In fact, Young-EOD and Mature-EOD had, respectively, the smallest and the largest number of DE genes (Fig. 4A). Neither showed a large overlap of the DE genes between MO and EOD (Fig. 4B). No more than 46 genes were significantly up- or down-regulated in both Young and Mature leaves at both time points (Fig. 4C). Lists of all DE genes are provided in Supplemental Data.

The genes up-regulated under FL were overrepresented by components of chloroplasts, whereas genes associated with DNA, ribosome, Golgi apparatus, and cell wall were enriched in the down-regulated genes (Supplemental Table S2). Some chloroplast components were also enriched in the down-regulated genes of Young-EOD. With regard to the biological processes of the DE genes, responses to light stimuli and vitamin metabolism were overrepresented in the up-regulated genes of Young and Mature leaves in MO, while photosynthesis and pigment metabolism were overrepresented in the up-regulated genes of Mature leaves at both time points (Supplemental Table S3). With regard to the down-regulated genes, enrichment was found for DNA replication, cell cycle, organelle fission and organization in Young-MO and for light harvesting and responses to light and other stimuli in Young-EOD.

Genes That Were Up- or Down-Regulated in All FL Samples

Figure 5 shows the 46 genes that were differentially expressed in all FL samples. Only three genes were down-regulated and the rest were up-regulated. Among the up-regulated genes was *LHCB7*, which is typically expressed in HL and EL (Kleine et al., 2007). Three CBC genes also underwent up-regulation in all FL samples (Fig. 5): one coding for CP12 protein (CP12-2), which mediates TRX-dependent reversible complex formation between phosphoribulokinase and glyceraldehyde-3-phosphate dehydrogenase; one for SEDOHEPTULOSE-1,7-BISPHOSPHATASE (SBPASE), which, like phosphoribulokinase and glyceraldehyde-3-phosphate dehydrogenase, is activated by reduced TRX in the light; and one for chloroplast FRUCTOSE-1,6-BISPHOSPHATE ALDOLASE1 (FBA1), which provides substrates for SBPASE and FRUCTOSE-1,6-BISPHOSPHATASE (FBPASE).

Oxygenation of RuBP by Rubisco triggers photorespiration in C_3 plants. Three genes encoding photorespiratory enzymes were up-regulated in all FL samples: GLYCOLATE OXIDASE1 (GOX1), which produces hydrogen peroxide (H_2O_2) in peroxisomes; CATALASE2 (CAT2), which detoxifies H_2O_2 therein; and the P protein of GLYCINE DECARBOXYLASE, which releases CO_2 in mitochondria (Fig. 5). In contrast to *CAT2*, *CAT3* was repressed under FL (Fig. 5). Increased gene expression was also found for BETA CARBONIC ANHYDRASE1 (BCA1), which interconverts CO_2 and

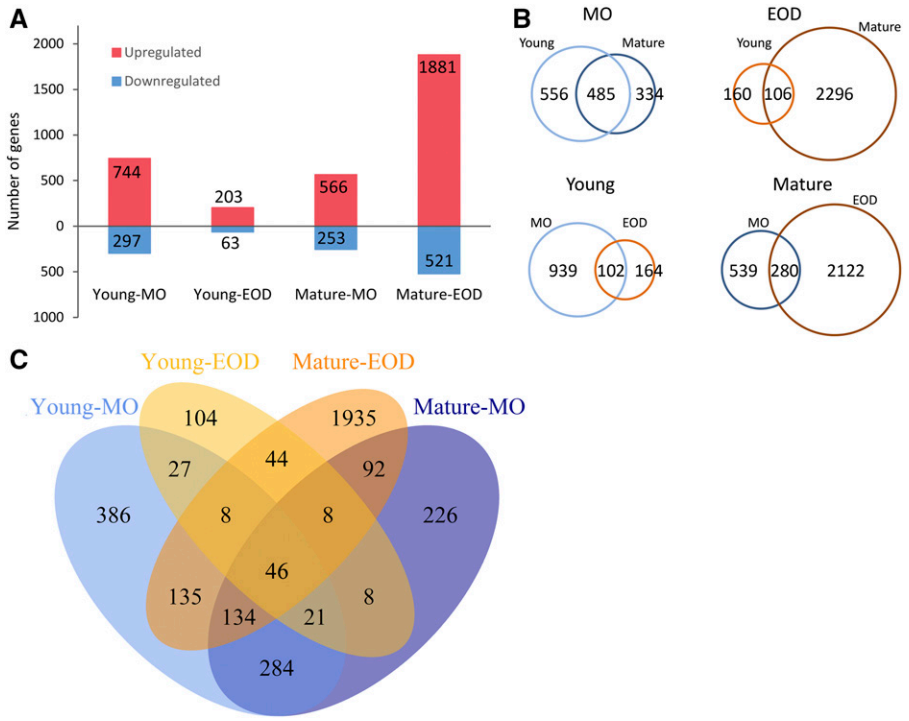

Figure 4. Comparison of transcriptomic responses of Young and Mature leaves in MO and at EOD after 3 d in the FL condition. Genes were regarded as DE genes when their fold change (FL/CL) values were ≥ 1.3 or ≤ 0.7. A, The number of up- and down-regulated genes. B, Pairwise comparisons of DE genes between Young and Mature leaves at the same time points (top) or between MO and EOD in the same leaves (bottom). C, Venn diagram illustrating the overlaps of DE genes in the four samples.

HCO_3^- in chloroplasts, and SUCROSE-PHOSPHATE SYNTHASE C, the second most abundant leaf sucrose-phosphate synthase isoform, which catalyzes a rate-limiting step in Suc synthesis.

The FL condition promoted the expression of three *ACTIVITY OF BC_1 COMPLEX KINASE* genes (Fig. 5) encoding ABC1K1, ABC1K5, and ABC1K6, all of which are localized in plastoglobuli. ABC1K1 phosphorylates tocopherol cyclase VITAMIN E1 (VTE1) in plastoglobuli (Martinis et al., 2014). In parallel, two *FATTY ACID DESATURASE* genes, *FAD4* and *FAD8*, were also up-regulated in all samples (Fig. 5). In chloroplasts, FAD4 provides trans-Δ^3-hexadecenoic acid (trans-16:1) for phosphatidylglycerol (PG) and FAD8 synthesizes α-linolenic acid (18:3 ω-3) for all glycerolipids but especially PG (Román et al., 2015). When liberated from membrane lipids, α-linolenic acid can be converted to 12-oxophytodienoic acid and jasmonic acid (JA), both of which can elicit defense responses in plants. The products of three *MES* (*METHYL ESTERASE*) genes, which were up-regulated under FL (Fig. 5), can demethylate methyl jasmonate (MeJA; MES16), methyl indole-3-acetic acid (MES16 and MES18), and *p*-nitrophenyl acetate (MES8) in vitro. In vivo, MES16 demethylates Chl catabolites (Christ et al., 2012).

Concomitant with the accumulation of antioxidants (Fig. 3, D and E; Supplemental Table S1), two pyridoxine (vitamin B_6) biosynthetic genes, *PDX1.1* (*PYRIDOXAL-5′-PHOSPHATE SYNTHASE1.1*) and *PDX1L4* (*PDX1-LIKE4*), were up-regulated in leaves under FL (Fig. 5). Pyridoxal 5′-phosphate (the active form of pyridoxine) is a cofactor of various enzymatic reactions, including photorespiratory Gly decarboxylation and the last step of Cys biosynthesis needed for the formation of glutathione, protein disulfide bonds, and iron-sulfur proteins. Pyridoxine and its derivatives are also able to scavenge $^1O_2$. All FL samples showed more than 4-fold up-regulation of *GPX7* (Fig. 5). Plant GPX catalyzes the reduction of H_2O_2 and lipid hydroperoxide to water and alcohol, respectively, using reduced TRX or glutathione as an e^- donor. Arabidopsis has two chloroplast GPX isoforms, GPX1 and GPX7, which play partially redundant roles in photooxidative stress (Chang et al., 2009).

BLUE-LIGHT INHIBITOR OF CRYPTOCHROMES1 (*BIC1*; Fig. 5) encodes a protein that inhibits light-induced dimerization and activation of the blue light and UV-A receptors cryptochromes (CRYs). In the nucleus, CRYs interact with COP1 (CONSTITUTIVE PHOTOMORPHOGENESIS 1)/SPA1 (SUPPRESSOR OF PHYTOCHROME A-105) ubiquitin ligase to suppress COP1-dependent degradation of light response-related transcription factors HY5 (LONG HYPOCOTYL5) and HYH (HY5 HOMOLOG). Heterodimers or homodimers of HY5 and HYH then bind to cis-acting DNA elements to regulate the transcription of photomorphogenic and light-responsive genes, including *BIC1* and *BIC2* (Wang et al., 2017). The FL samples had higher transcript levels of *HYH* (Fig. 5), which is functionally similar to, but not identical with, *HY5* (Brown and Jenkins, 2008). Conversely, a B box transcription factor gene, *BBX17*, was down-regulated in all samples in the FL condition (Fig. 5). Some members of the BBX family proteins interact with COP1, HY5, and HYH to regulate photomorphogenesis, while others are associated with flowering control and stress responses (Gangappa and Botto, 2014).

The DE genes in Figure 5 suggest adjustments of various cellular processes during long-term acclimation to the FL condition. Yet, these are only a small fraction

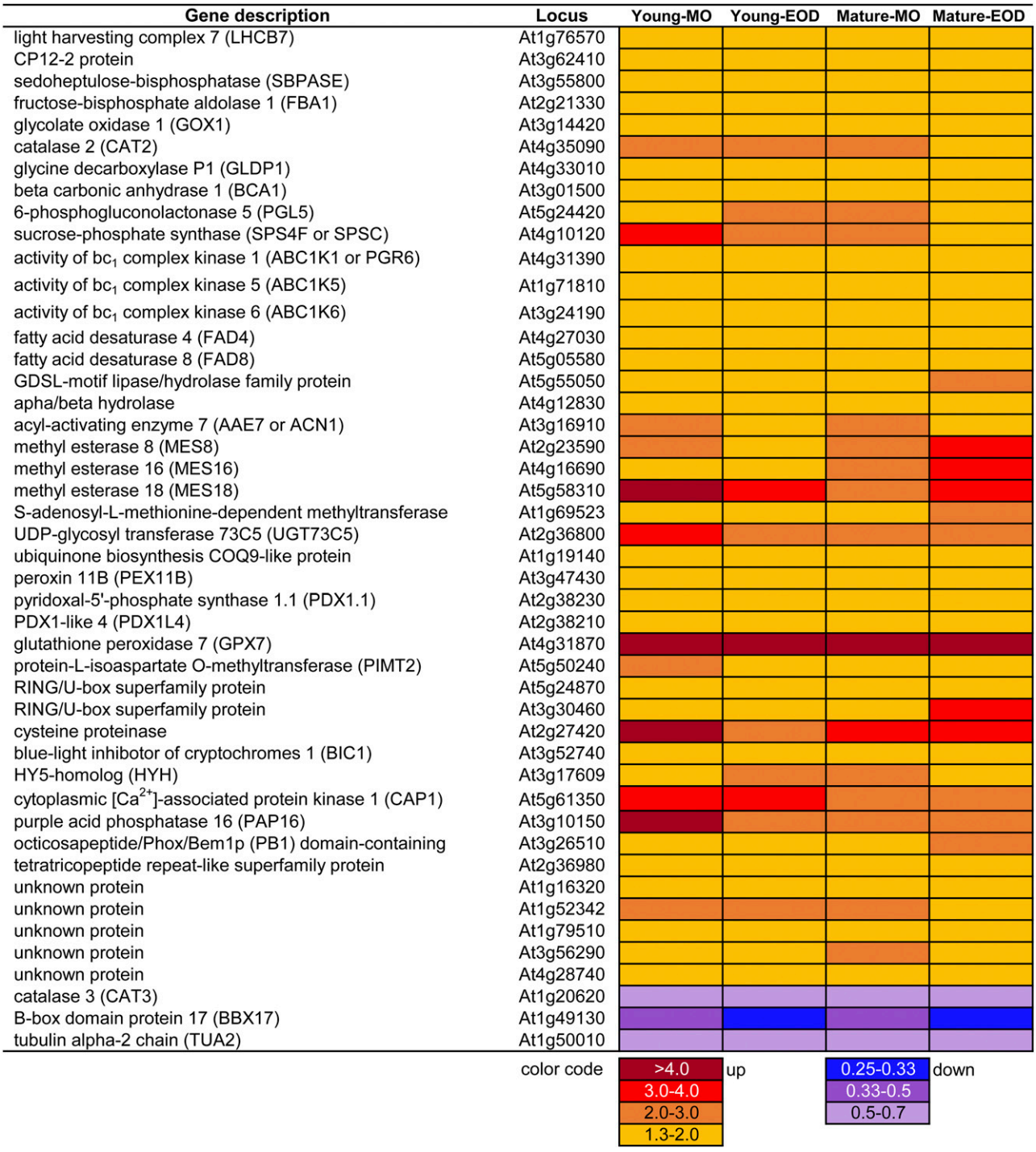

Figure 5. Genes that were differentially expressed in all samples between FL and CL on day 3.

of the DE genes identified under FL (Fig. 4C). In the following sections, we explore genes that were significantly up- or down-regulated in not all but some of the FL samples (but always with statistical significance based on the biological replicates), focusing on highly up-regulated genes (FL/CL $\geq$ 4) and genes that are related to photosynthesis and pigment metabolism.

Highly Up-Regulated Genes under FL

Fewer than 30 genes were up-regulated by 4-fold or greater in any of the FL samples on day 3 (Supplemental Fig. S2). Since some of these genes were associated with biotic stress responses, we checked their expression in publicly available Arabidopsis leaf transcriptome

data sets studying biotic stress and hormone responses. Nine genes, which were highly up-regulated under FL but not found in the public data sets, are listed in Supplemental Table S4.

The expression patterns of our highly up-regulated genes revealed a clear contrast between Young and Mature leaves in terms of their responses to biotic stress and hormone treatments (Supplemental Fig. S4). About half of the genes, which were highly up-regulated in Young leaves under FL (the first three columns from the left; Supplemental Fig. S4, A and B), were also strongly induced in systemic (nontreated) leaves 2 d after inoculation with *Pseudomonas syringae* pv *maculicola* (*Psm*; SAR 48 h; the fourth column) and in the constitutive SAR mutant *cpr5* (*constitutive expressor of pathogenesis related genes5*; the fifth column). The highly up-regulated genes of Mature leaves (Supplemental Fig. S4, C and D), on the other hand, did not respond to SAR. To evaluate the similarity of gene expression, a mean fold change of the highly up-regulated genes was calculated for each data set (i.e. for each column of Supplemental Fig. S4) and summarized in Figure 6. The SAR 48 h and *cpr5*/Col data sets had very high mean fold change values (greater than 10- or 20-fold) for the highly up-regulated genes of Young leaves. While high mean values (greater than 4-fold) were also found for the genes of Young-EOD in the JA-dependent response to *Psm* (Col/*coi1* [*coronate insensitive1*]) and the SA 2-h or MeJA 3-h treatment, these were attributable to very strong up-regulation of a few genes (Supplemental Fig. S4B).

Since SA is a major endogenous signal for SAR induction and since SA accumulation is also associated with plastid-to-nucleus retrograde signaling via MEcPP or β-cyclocitral (Xiao et al., 2012; Lv et al., 2015), we analyzed SA contents in leaves on day 3. Low levels of SA and SA glucosides were detected under both FL and CL conditions, with twice as much SA found in Young leaves as in Mature leaves (Supplemental Fig. S5, A and B). In contrast to the responses of SAR-like genes in Young leaves, however, the levels of SA and SA glucosides were unchanged or even reduced under FL. Pipecolic acid (Pip), an L-Lys-derived nonprotein amino acid (Hartmann et al., 2017), is another SAR regulatory metabolite that accumulates in response to pathogen inoculation (Návarová et al., 2012). Unlike in the case of SA, FL tended to promote Pip accumulation in both Young and Mature leaves but especially the latter (Supplemental Fig. S5C). The levels of JA were below the detection limit in all samples.

Differentially Regulated Genes in Photoprotection, Photosynthesis, and Photorespiration

As shown by the enrichment of photosynthesis and chloroplast components in the DE genes (Supplemental Tables S2 and S3), a large number of photoprotective, photosynthetic, and photorespiratory genes were responding to FL in different samples (Fig. 7). Most of these genes were up-regulated under FL, with the exception of *LHCBs* and a gene for a 5-kD PSII protein, which were down-regulated in Young-EOD. All but Young-EOD had increased transcript levels of *PSBS* and *KEA1* (*K$^+$ EFFLUX ANTIPORTER1*), which encodes a K^+/H^+ antiporter in the chloroplast inner envelop. As for the thylakoid-localized KEA3, gene expression was enhanced in Mature leaves at both time points (Fig. 7). Up-regulation under FL was also found for *ELIP1* and *ELIP2* especially in MO.

As the decrease in linear e^- transport and increase in NPQ were detected in the FL plants (Fig. 2, B and C), genes related to CEF underwent concomitant up-regulation in Mature-EOD (Fig. 7). Many genes associated with NADPH dehydrogenase (NDH)-like complex were up-regulated in concert, together with *LHCA5* and *LHCA6*, which are needed for the formation of the NDH-PSI supercomplex. Also, components of the other CEF pathway (PGR5 [PROTON GRADIENT REGULATION5], PGRL1A [PGR5-LIKE1A], and PGRL1B) showed increased gene expression in Mature-EOD. Up-regulated in Mature-EOD were also the Rieske iron-sulfur protein gene *PETC* (*PHOTOSYNTHETIC ELECTRON TRANSFER C*) and *PETM* of Cyt

Sample	FL/CL	SAR 48 h	*cpr5*/Col	*Psm* 24 h	Col/*sid2*	Col/*coi1*	Col/*ein2*	SA 2 h	MeJA 3 h	H_2O_2 1 h	ABA 3 h	IAA 3 h	flg22 4 h
Young-MO	6.71	11.87	13.09	2.14	1.74	1.02	0.89	3.13	1.03	3.84	1.60	1.15	1.74
Mature-MO	7.55	0.81	0.64	1.02	0.96	1.24	1.31	0.89	0.96	1.39	2.89	0.75	0.97
Young-EOD	11.36	22.19	19.48	1.31	1.58	4.53	0.87	4.08	4.05	1.32	1.73	0.88	1.29
Mature-EOD	5.98	0.67	0.78	1.46	0.62	1.27	1.09	0.67	0.75	1.06	1.17	1.11	2.04

Figure 6. Mean fold change values of the highly up-regulated genes (FL/CL $\geq$ 4) in publicly available Arabidopsis transcriptome data sets studying biotic stress and hormone responses. The numbers in the cells are color coded from black (little change or down-regulation) to red (strong up-regulation). The fold change values of individual genes are shown in Supplemental Figure S4. The treatments are as follows: SAR 48 h, systemic (nontreated) leaves of the wild-type Col-0 plants 2 d after inoculation with *Psm* (*Pseudomonas syringae* pv. *maculicola*) versus mock; *cpr5*/Col, *cpr5* (*constitutive expressor of pathogenesis related gene5*) mutant versus Col; *Psm* 24 h, local (treated) leaves of Col-0 plants 1 d after inoculation with *Psm* versus mock; Col/*sid2* (*salicylic acid induction deficient2*), Col/*coi1* (*coronate insensitive1*), or Col/*ein2* (*ethylene insensitive2*), Col versus SA-deficient or JA- and ethylene-insensitive mutants 1 d after inoculation with *Psm*; SA 2 h, 2 h after spraying with 1 mM SA versus mock; MeJA 3 h, 3 h after treatment with 10 μM MeJA versus mock; H_2O_2 1 h, 1 h after application of 20 mM H_2O_2 versus mock; ABA (abscisic acid) 3 h, 3 h after treatment with 10 μM ABA versus mock; IAA (indole acetic acid) 3 h, 3 h after treatment with 1 μM IAA versus mock; flg22 (22-mer peptide of the elicitor-active domain of bacterial flagellin) 4 h, 4 h after treatment with 1 mM flg22 versus mock.

Gene description	Locus	Young-MO	Young-EOD	Mature-MO	Mature-EOD
Light reaction-related					
PSII 5 kD protein	At1g51400				
PSII light harvesting complex 1.1 (LHCB1.1)	At1g29920				
PSII light harvesting complex 1.2 (LHCB1.2)	At1g29910				
PSII light harvesting complex 1.3 (LHCB1.3)	At1g29930				
PSII light harvesting complex 1.4 (LHCB1.4)	At2g34430				
PSII light harvesting complex 1.5 (LHCB1.5)	At2g34420				
PSII light harvesting complex 2.1 (LHCB2.1)	At2g05100				
PSII light harvesting complex 2.2 (LHCB2.2)	At2g05070				
PSII light harvesting complex 2.3 (LHCB2.3)	At3g27690				
PSII light harvesting complex 3 (LHCB3)	At5g54270				
PSII light harvesting complex 4.2 (LHCB4.2)	At3g08940				
PSII light harvesting complex 6 (LHCB6)	At1g15820				
light harvesting complex 7 (LHCB7)	**At1g76570**				
PSBS protein, non-photochemical quenching 4 (NPQ4)	**At1g44575**				
K^+ efflux antiporter 1 (KEA1)	**At1g01790**				
K^+ efflux antiporter 3 (KEA3)	At4g04850				
early light-induced protein 1 (ELIP1)	**At3g22840**				
early light-induced protein 2 (ELIP2)	At4g14690				
PSII subunit O 2 (PSBO2 or OEC33)	At3g50820				
PSBP-like protein 1 (PPL1)	At3g55330				
PSBP domain-containing protein 3 (PPD3)	At1g76450				
PSII reaction center subunit W (PSBW)	At2g30570				
one helix protein (OHP)	At5g02120				
low PSII accumulation 19 (LPA19 or PSB27-H1)	At1g05385				
PSI subunit N (PSAN)	At5g64040				
PSI subunit P (PSAP)	At2g46820				
PSI light harvesting complex 5 (LHCA5)	At1g45474				
PSI light harvesting complex 6 (LHCA6)	At1g19150				
NDH-like complex L (NDHL or CRR23)	At1g70760				
NDH-like complex M (NDHM)	**At4g37925**				
NDH-like complex N (NDHN)	**At5g58260**				
NDH-like complex O (NDHO)	At1g74880				
NDH-like complex B1 (PNSB1, NDH48 or NDF1)	At1g15980				
NDH-like complex B2 (PNSB2, NDH45 or NDF2)	**At1g64770**				
NDH-like complex B3 (PNSB3 or NDF4)	At3g16250				
NDH-like complex B4 (PNSB4 or NDF6)	At1g18730				
NDH-like complex B5 (PNSB5 or NDH18)	At5g43750				
NDH-like complex L3 (PNSL3)	At3g01440				
NDH-like complex L1 (PNSL1 or PPL2)	At2g39470				
NDH-like complex L2 (PNSL2)	At1g14150				
NDH-like complex L4 (PNSL4) or FKBP16-2	At4g39710				
NDH-like complex L5 (PNSL5) or cyclophilin 20-2	At5g13120				
NDH-like complex T (NDHT or CRRJ)	**At4g09350**				
NDH-like complex U (NDHU or CRRL)	At5g21430				
PSBQ-like 3 (PQL3)	At2g01918				
chlororespiratory reduction 1 (CRR1 or DHPR-like)	At5g52100				
chlororespiratory reduction 3 (CRR3)	At2g01590				
chlororespiratory reduction 6 (CRR6)	At2g47910				
chlororespiratory reduction 7 (CRR7)	At5g39210				
NDH-dependent cyclic electron flow 5 (NDF5 or PNSB2 homolog)	At1g55370				
post-illumination chlorophyll fluorescence increase (PIFI)	At3g15840				
proton gradient regulation 5 (PGR5)	At2g05620				
PGR5-like 1A (PGRL1A)	At4g22890				
PGR5-like 1B (PGRL1B)	At4g11960				
calcium sensing receptor (CAS)	At5g23060				
photosynthetic electron transfer C (PETC)	At4g03280				
photosynthetic electron transfer M (PETM)	At2g26500				
ATP synthase Fo b/b' subunit (PDE334)	At4g32260				
ATP synthase F1 gamma subunit (ATPC1)	At4g04640				
ATP synthase Fo assembly protein (CGL160)	At2g31040				
STN7 kinase	At1g68830				
chloroplast sensor kinase (CSK)	At1g67840				
ferredoxin 1 (FD1)	At1g10960				
ferredoxin 2 (FD2)	At1g60950				

(Table continues on the following page.)

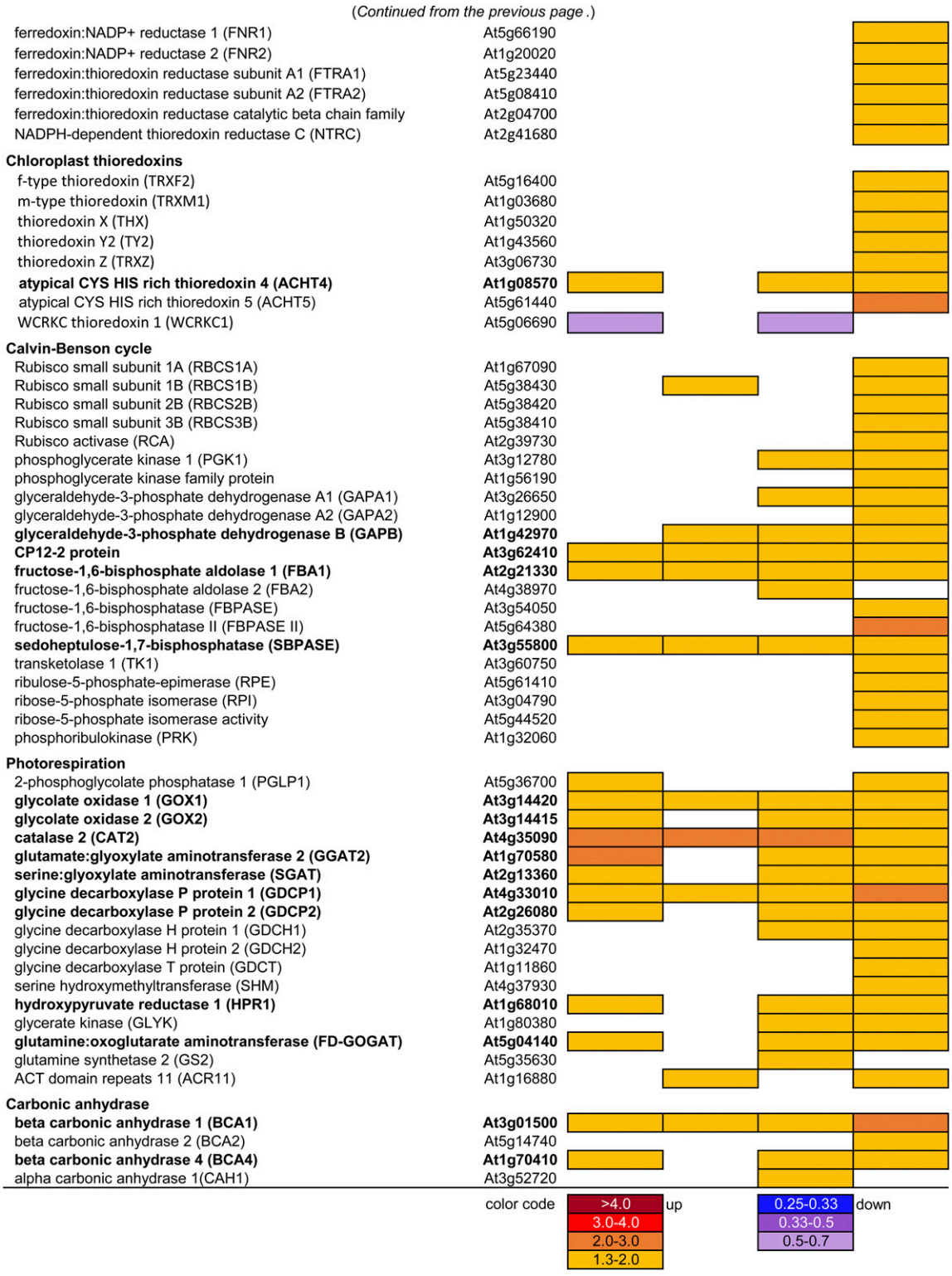

Figure 7. DE genes related to photoprotection, photosynthesis, and photorespiration. White cells indicate that data did not fulfill the filtering criteria based on CPM, FDR, and the ratio between the FL and CL conditions (FL/CL). Genes that were differentially expressed in three or four samples (i.e. three or four out of Young-MO, Young-EOD, Mature-MO, and Mature-EOD) are written in boldface.

b_6f, ATP synthase subunit genes *ATPC1* and *PIGMENT DEFECTIVE334*, as well as the assembly component *CONSERVED ONLY IN THE GREEN LINEAGE160* (Fig. 7). Furthermore, the FL treatment enhanced the gene expression of STN7 and CHLOROPLAST SENSOR KINASE, which, in response to the PQ pool reduction, facilitate balancing of PSII and PSI excitation via LHCII phosphorylation and gene transcription.

The iron-sulfur protein FD mediates e^- transfer from PSI to FD:$NADP^+$ REDUCTASE (FNR), CEF, and various chloroplast redox and metabolic pathways. Both minor (*FD1*) and major (*FD2*) leaf-type *FD* genes of Arabidopsis were up-regulated under FL but at different time points (Fig. 7). Furthermore, Mature-EOD had increased expression of leaf *FNR* (*FNR1* and *FNR2*), *FD: TRX REDUCTASE*, and multiple chloroplast *TRX* genes, including *ATYPICAL CYS HIS RICH TRX4*. The stroma thylakoid-localized *ATYPICAL CYS HIS RICH TRX4*, together with 2-Cys peroxiredoxin, transduces oxidative signals to inactivate the first enzyme of starch synthesis and thereby counteracts reductive activation signals from other TRXs (Geigenberger et al., 2017). The redox signals thus transduced are thought to fine-tune the enzyme activity under FL conditions.

While J_{max} and V_{cmax} did not change (Fig. 2D), genes in the CBC manifested parallel up-regulation in Mature leaves after 3 d under FL. Starting from Rubisco small subunits (RBCS) and Rubisco activase, all CBC enzymes except triose phosphate isomerase are found in Figure 7. Marked co-up-regulation under FL was also seen for photorespiratory genes, including GLUTAMINE:OXOGLUTARATE AMINOTRANSFERASE, GLUTAMINE SYNTHETASE2, and its activator ACT DOMAIN REPEATS11 for ammonia reassimilation. Besides, three samples had increased transcript levels of *BCA1* and *BCA4* (Fig. 7); BCA1 in chloroplasts and BCA4 in the plasma membrane are thought to coregulate intracellular [HCO_3^-] and CO_2-induced guard cell movements (Hu et al., 2015).

Differentially Regulated Genes in Pigment and Prenylquinone Metabolism

The overrepresentation of pigment metabolism in the DE genes of Mature leaves (Supplemental Table S3) prompted us to examine gene expression responses in tetrapyrrole, carotenoid, and prenylquinone metabolism. Six genes in the initial part of tetrapyrrole biosynthesis were up-regulated in Mature-EOD (Fig. 8), including *GLUTR1*, which codes for redox-regulated GLUTAMYL TRNA REDUCTASE at the first committed step of tetrapyrrole biosynthesis, and *GLUTRBP*, which codes for thylakoid-localized GLUTR-BINDING PROTEIN.

In the Chl biosynthetic pathway, *NADPH:PROTOCHLOROPHYLLIDE OXIDOREDUCTASE A* (*PORA*) and *PORB* were strongly down-regulated in the FL condition (Fig. 8). Arabidopsis has three POR isozymes that catalyze light-dependent reduction of protochlorophyllide to chlorophyllide *a*; PORA and PORB are active during early stages of greening, whereas PORB and PORC may maintain Chl in green leaves (Frick et al., 2003; Masuda et al., 2003). In contrast to *PORA* and *PORB*, *PORC* showed enhanced expression under FL in Mature-EOD, together with several other genes in Chl biosynthesis, such as *GENOMES UNCOUPLED5*, which encodes the H subunit of Mg chelatase associated with retrograde signaling (Mochizuki et al., 2001). Although the plants were similarly green under FL and CL on day 3 (Figs. 1A and 3C), longer FL exposure reduces Chl contents (Alter et al., 2012; Caliandro et al., 2013). In accordance, we found concomitant up-regulation of the Chl breakdown genes *NON-YELLOW COLORING1*, *STAY-GREEN1*, *CHLOROPHYLL DEPHYTYLASE1*, *PHYTYL ESTER SYNTHASE1*, *RED CHLOROPHYLL CATABOLITE REDUCTASE*, *TRANSLOCON AT THE INNER ENVELOPE MEMBRANE OF CHLOROPLASTS55*, and *MES16* (Fig. 8).

FERROCHELATASE2 is involved in the synthesis of heme-containing Cyt b_6f. Since heme harbors redox-active Fe, which can produce highly reactive hydroxyl radicals from H_2O_2, accumulation of free heme should be avoided. Chloroplast-localized HEME-BINDING PROTEIN5 (HBP5) binds heme and interacts with HEME OXYGENASE1 to regulate heme metabolism (Lee et al., 2012). The three genes *FERROCHELATASE2*, *HBP5*, and *HEME OXYGENASE1* were up-regulated together in Mature-EOD (Fig. 8). The MO samples, on the other hand, had increased transcripts of *HBP1* encoding a putative tetrapyrrole carrier protein found in cytoplasm and around the nucleus.

Mature leaves showed concerted up-regulation of genes in the MEP and carotenoid biosynthetic pathways, especially at EOD (Fig. 8). In Arabidopsis, GERANYLGERANYL DIPHOSPHATE SYNTHASE11 supports the synthesis of carotenoids and isoprenoid side chains of Chls, PQ, and tocopherols (Ruiz-Sola et al., 2016). While Mature leaves had increased transcript levels of *GERANYLGERANYL DIPHOSPHATE SYNTHASE11* and several carotenogenic genes such as *ZEAXANTHIN EPOXIDASE* (*ZEP*) and *VDE* in the xanthophyll cycle, two *B-CAROTENE HYDROXYLASE* genes, *BCH1* and *BCH2*, were the only DE genes of this pathway identified in Young leaves (Fig. 8). The two BCH enzymes primarily catalyze hydroxylation of β-carotene to produce zeaxanthin. With regard to apocarotenoid metabolism, FL up-regulated *B-CAROTENE ISOMERASE* (*DWARF27*), *CAROTENOID CLEAVAGE DIOXYGENASE1* (*CCD1*), and *CCD4* while repressing two genes in ABA and strigolactone biosynthesis at EOD, namely, *ABA DEFICIENT2* in Young leaves and *MORE AXILLARY BRANCHES1* in Mature leaves.

All DE genes in prenylquinone biosynthesis were up-regulated under FL, mostly in MO (Fig. 8). Enhanced gene expression was found for *TYROSINE AMINOTRANSFERASE1* and *4-HYDROXYPHENYLPYRUVATE DIOXYGENASE*, which are involved in homogentisate

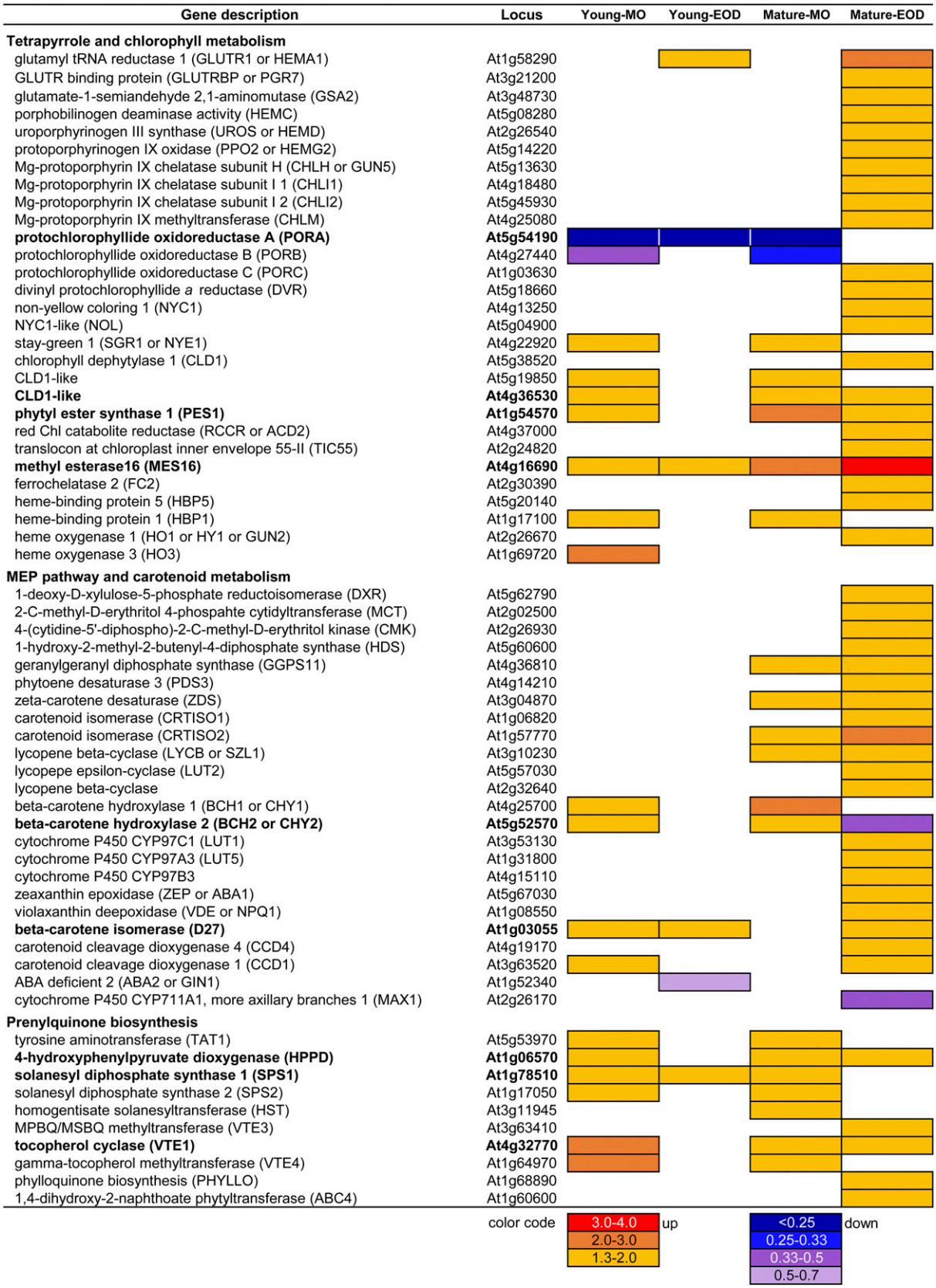
Gene description
Locus
Young-MO
Young-EOD
Mature-MO
Mature-EOD
Tetrapyrrole and chlorophyll metabolism
glutamyl tRNA reductase 1 (GLUTR1 or HEMA1) At1g58290
GLUTR binding protein (GLUTRBP or PGR7) At3g21200
glutamate-1-semiandehyde 2,1-aminomutase (GSA2) At3g48730
porphobilinogen deaminase activity (HEMC) At5g08280
uroporphyrinogen III synthase (UROS or HEMD) At2g26540
protoporphyrinogen IX oxidase (PPO2 or HEMG2) At5g14220
Mg-protoporphyrin IX chelatase subunit H (CHLH or GUN5) At5g13630
Mg-protoporphyrin IX chelatase subunit I 1 (CHLI1) At4g18480
Mg-protoporphyrin IX chelatase subunit I 2 (CHLI2) At5g45930
Mg-protoporphyrin IX methyltransferase (CHLM) At4g25080
protochlorophyllide oxidoreductase A (PORA) At5g54190
protochlorophyllide oxidoreductase B (PORB) At4g27440
protochlorophyllide oxidoreductase C (PORC) At1g03630
divinyl protochlorophyllide a reductase (DVR) At5g18660
non-yellow coloring 1 (NYC1) At4g13250
NYC1-like (NOL) At5g04900
stay-green 1 (SGR1 or NYE1) At4g22920
chlorophyll dephytylase 1 (CLD1) At5g38520
CLD1-like At5g19850
CLD1-like At4g36530
phytyl ester synthase 1 (PES1) At1g54570
red Chl catabolite reductase (RCCR or ACD2) At4g37000
translocon at chloroplast inner envelope 55-II (TIC55) At2g24820
methyl esterase16 (MES16) At4g16690
ferrochelatase 2 (FC2) At2g30390
heme-binding protein 5 (HBP5) At5g20140
heme-binding protein 1 (HBP1) At1g17100
heme oxygenase 1 (HO1 or HY1 or GUN2) At2g26670
heme oxygenase 3 (HO3) At1g69720
MEP pathway and carotenoid metabolism
1-deoxy-D-xylulose-5-phosphate reductoisomerase (DXR) At5g62790
2-C-methyl-D-erythritol 4-phospahte cytidyltransferase (MCT) At2g02500
4-(cytidine-5'-diphospho)-2-C-methyl-D-erythritol kinase (CMK) At2g26930
1-hydroxy-2-methyl-2-butenyl-4-diphosphate synthase (HDS) At5g60600
geranylgeranyl diphosphate synthase (GGPS11) At4g36810
phytoene desaturase 3 (PDS3) At4g14210
zeta-carotene desaturase (ZDS) At3g04870
carotenoid isomerase (CRTISO1) At1g06820
carotenoid isomerase (CRTISO2) At1g57770
lycopene beta-cyclase (LYCB or SZL1) At3g10230
lycopepe epsilon-cyclase (LUT2) At5g57030
lycopene beta-cyclase At2g32640
beta-carotene hydroxylase 1 (BCH1 or CHY1) At4g25700
beta-carotene hydroxylase 2 (BCH2 or CHY2) At5g52570
cytochrome P450 CYP97C1 (LUT1) At3g53130
cytochrome P450 CYP97A3 (LUT5) At1g31800
cytochrome P450 CYP97B3 At4g15110
zeaxanthin epoxidase (ZEP or ABA1) At5g67030
violaxanthin deepoxidase (VDE or NPQ1) At1g08550
beta-carotene isomerase (D27) At1g03055
carotenoid cleavage dioxygenase 4 (CCD4) At4g19170
carotenoid cleavage dioxygenase 1 (CCD1) At3g63520
ABA deficient 2 (ABA2 or GIN1) At1g52340
cytochrome P450 CYP711A1, more axillary branches 1 (MAX1) At2g26170
Prenylquinone biosynthesis
tyrosine aminotransferase (TAT1) At5g53970
4-hydroxyphenylpyruvate dioxygenase (HPPD) At1g06570
solanesyl diphosphate synthase 1 (SPS1) At1g78510
solanesyl diphosphate synthase 2 (SPS2) At1g17050
homogentisate solanesyltransferase (HST) At3g11945
MPBQ/MSBQ methyltransferase (VTE3) At3g63410
tocopherol cyclase (VTE1) At4g32770
gamma-tocopherol methyltransferase (VTE4) At1g64970
phylloquinone biosynthesis (PHYLLO) At1g68890
1,4-dihydroxy-2-naphthoate phytyltransferase (ABC4) At1g60600
color code
3.0-4.0
2.0-3.0
1.3-2.0
up
<0.25
0.25-0.33
0.33-0.5
0.5-0.7
down

biosynthesis for PQ and tocopherols; *SOLANESYL DIPHOSPHATE SYNTHASE1* (*SPS1*) and *SPS2*, which provide isoprenoid side chains for ubiquinone and PQ; and *VTE1* and *VTE4*, which are involved in tocopherol and plastochromanol biosynthesis. Increased accumulation of α-tocopherol, reduced PQ (PQH_2), and plastochromanol, all of which can serve as antioxidants, have been reported in Arabidopsis leaves under HL (Dłużewska et al., 2015). We also found up-regulation of two phylloquinone (vitamin K_1) biosynthetic genes, *PHYLLO* and *ABERRANT CHLOROPLAST DEVELOPMENT4*, in Mature-EOD (Fig. 8). Inside PSI, phylloquinone mediates e^- transfer from Chl A_0 to the first iron-sulfur cluster F_x.

Response of Cyclic Gene Expression to FL

The concomitant responses of functionally related DE genes (Figs. 5, 7, and 8) point to their coregulation, whereas the limited overlaps found between the DE genes of Young and Mature leaves in MO and at EOD (Fig. 4) indicate interactions between FL, leaf development stage, and diurnal processes. In particular, the distinct FL responses observed in MO and at EOD (Fig. 4B) are suggestive of time of day-dependent transcriptional regulation by the circadian clock, the molecular timekeeper of the cell. Indeed, 38% to 50% of our DE genes show light/dark cyclic expression in leaves, and 42% to 58% are classified as circadian regulated, since they maintain cyclic expression in continuous light (light/light; Fig. 9A; see Supplemental Data for DE cyclic genes). Interestingly, most of the light/dark cyclic genes, which were up-regulated under FL in MO, are morning genes in the light/dark condition, peaking between dawn and midday (Fig. 9B). In clear contrast, those that were down-regulated under FL in MO are evening genes. While the number of the DE cyclic genes was too small to infer peak phase distribution in Young-EOD, the pattern in Mature-EOD was similar to those found in MO, except that there was an additional cluster of up-regulated evening genes (Fig. 9B).

Seeing the opposite FL responses of morning and evening genes, we examined the biological processes of these genes. For this analysis, the DE genes peaking at Zeitgeber time (ZT) 21 to ZT6 were grouped together as morning genes and those peaking at ZT8 to ZT16 as evening genes; ZT0 is defined as the time when the light is turned on. Many DE cyclic genes are associated with synthesis, modification, and degradation of RNAs and proteins (Fig. 9C). Nearly all DE morning genes in these processes were up-regulated under FL, whereas the DE evening genes were mostly down-regulated in MO and up-regulated in Mature-EOD. Similar patterns were also found for the genes in carbohydrate and secondary metabolism or redox and signaling. The genes predominantly down-regulated under FL were growth-related evening genes involved in processes such as DNA synthesis and organization, cell division, and development of cytoskeleton and cell wall (Fig. 9C), in keeping with the overrepresentation of these processes in the down-regulated genes of Young-MO (Supplemental Table S3).

Changes in the expression of cyclic genes observed at two particular time points could be caused by (1) altered amplitude of oscillation or (2) a shift of peak expression time. To determine which of these scenarios can explain the observation for FL, we analyzed day-night (diel) expression of four DE cyclic genes (*LHCB1.2*, *CAT2*, *ELIP2*, and *GPX7*) in Young and Mature leaves on day 1 and day 3. Two highly expressed genes in leaves, *LHCB1.2* and *CAT2*, were repressed or enhanced, respectively, under FL on both days (Supplemental Fig. S6, A–D), confirming qualitatively the transcriptome data (Figs. 5 and 7). Their peak expression time seemed to change slightly from day 1 to day 3, but this was observed in both conditions. Two stress-responsive genes, *ELIP2* and *GPX7*, underwent strong up-regulation under FL (Supplemental Fig. S6, E–H), as shown by RNA-Seq (Figs. 5 and 7). While the expression of *ELIP2* declined from day 1 to day 3, it remained high for *GPX7*. Together, these results support altered amplitude of cyclic gene expression under FL.

Many components of the central clock oscillator were among the DE cyclic genes under FL. Both morning and evening component genes were up-regulated in their respective phases, namely, Myb transcription factor genes *CCA1* (*CIRCADIAN CLOCK ASSOCIATED1*) and *LATE ELONGATED HYPOCOTYL* in MO and transcriptional repressor genes *PRR7* (*PSEUDO-RESPONSE REGULATOR7*), *PRR5*, *PRR3*, and *TOC1* (*TIMING OF CAB EXPRESSION1*) together with *ELF3* (*EARLY FLOWERING3*) and *ELF4* at EOD (Supplemental Figs. S6, I–L, and S7). Three samples had increased transcript levels of the light- and stress-responsive gene *SIGMA FACTOR5* (*SIG5*), encoding a plastid RNA polymerase subunit that regulates transcription of the PSII D2 protein gene *psbD*. Although SIG5 is not a component but an output of the clock, its cyclic gene expression coordinates chloroplast transcription with circadian regulation of nuclear transcription (Noordally et al., 2013). We also found up-regulation of *SIG4* in Mature-EOD (Supplemental Fig. S7), in which many genes of the NDH-like complex were concurrently

Figure 8. DE genes related to the metabolism of photosynthetic pigments and prenylquinones. White cells indicate that data did not fulfill the filtering criteria based on CPM, FDR, and the ratio between the FL and CL conditions (FL/CL). Genes that were differentially expressed in three or four samples (i.e. three or four out of Young-MO, Young-EOD, Mature-MO, and Mature-EOD) are written in boldface.

A

Number of genes		Cyclic in light/dark	Cyclic in continuous light	Cyclic in both
Young-MO	1041	497 (47.7%)	534 (51.3%)	332 (31.9%)
Young-EOD	266	108 (40.6%)	123 (46.2%)	75 (28.2%)
Mature-MO	819	414 (50.5%)	477 (58.2%)	302 (36.9%)
Mature-EOD	2402	914 (38.1%)	1007 (41.9%)	520 (21.6%)

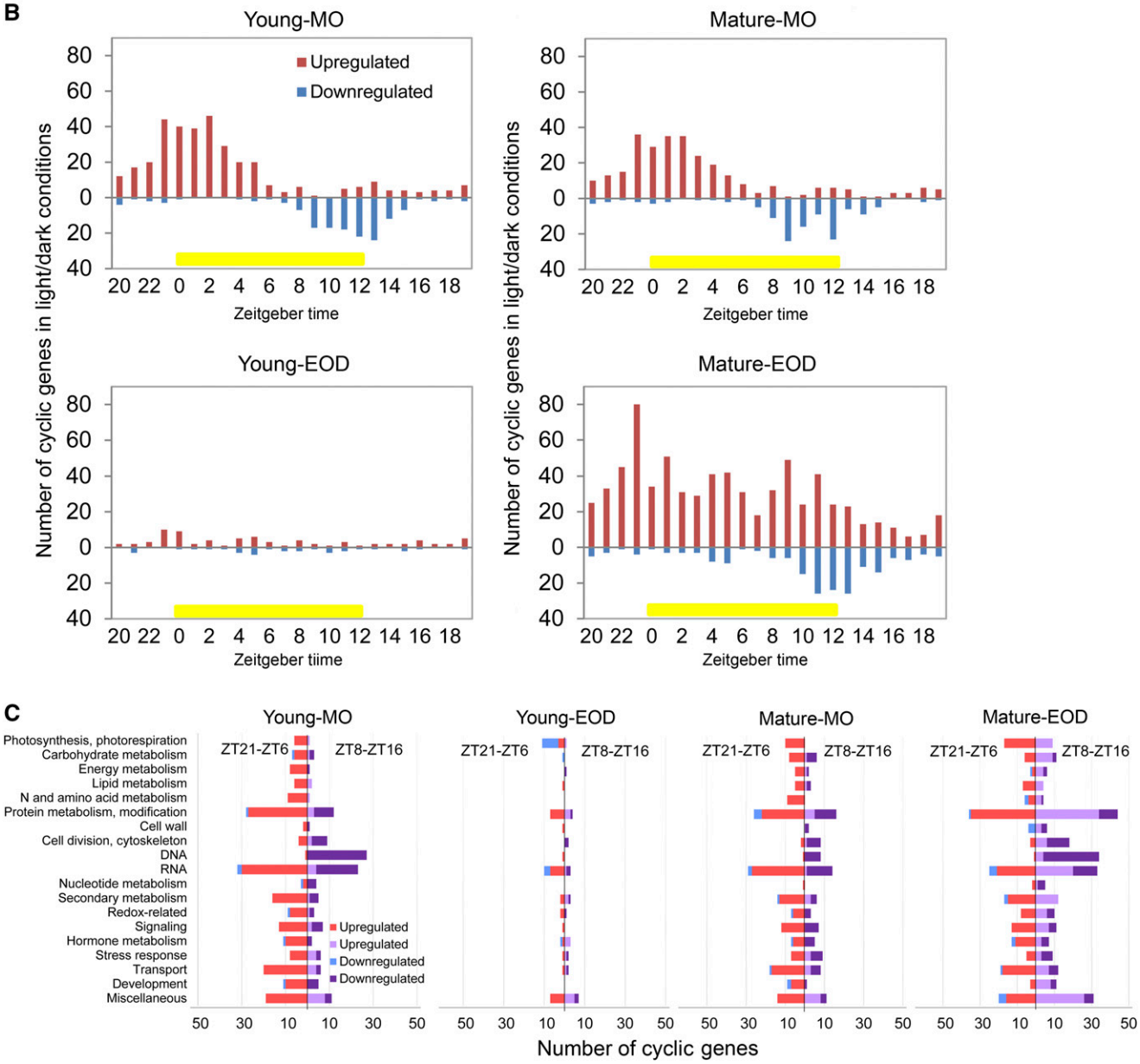

Figure 9. DE cyclic genes in the FL condition. A, The numbers of DE genes that are classified as cyclic in 12-h/12-h light/dark conditions, in continuous light (circadian) conditions, and in both conditions. B, Peak phase distribution of the DE light/dark cyclic genes in the four samples. The numbers of up- and down-regulated cyclic genes were counted separately according to their peaking time in 12-h/12-h light/dark conditions. Zeitgeber time zero (ZT0) is defined as the time when the light was turned on in the climate chamber. Yellow bars denote the light period. C, Biological processes of the DE light/dark cyclic genes peaking at ZT21 to ZT6 and ZT8 to ZT16. Energy metabolism includes glycolysis, citric acid cycle, and mitochondrial electron transport. Cofactor and vitamin biosynthesis are included in secondary metabolism. The data in C do not include genes that are not assigned to any cellular processes.

Table 1. *Consensus sequence motifs enriched in upstream regions of DE light/dark cyclic genes*

The numbers show fold enrichment compared with the genome-wide occurrence. The percentage score gives the proportion of genes having the motif in the gene set of each sample. The total number of the DE light/dark cyclic genes is indicated in parentheses after the sample name. The ACGT core is underlined for ACGT-containing motifs. The International Union of Pure and Applied Chemistry nucleotide ambiguity codes are as follows: M, A or C; N, A or C or G or T; R, A or G; Y, C or T. Dashes (–) denote no significant enrichment of the corresponding motifs.

Motif	Young-MO (497 Genes)	Young-EOD (108 Genes)	Mature-MO (414 Genes)	Mature-EOD (914 Genes)
I box-like				
CTTATCCN	2.29 (3%)	4.31 (6%)	3.23 (5%)	2.71 (4%)
ACGT-containing				
G box				
CACGTGGC	2.36 (8%)	–	2.53 (8%)	–
MCACGTGGC	2.33 (6%)	–	2.35 (6%)	–
CACGTGTA	2.05 (6%)	–	2.13 (6%)	–
G box- or Z box-like				
RYACGTGGYR	2.17 (5%)	–	2.40 (6%)	–
YACGTGGC	2.14 (10%)	–	2.05 (10%)	–
Z box-like				
TACGTGGA	2.04 (3%)	3.83 (6%)	–	–
Hex, TGA box				
TGACGTGGC	2.53 (3%)	–	2.32 (3%)	2.75 (4%)
TGACGTGG	2.50 (7%)	–	2.33 (7%)	2.15 (6%)
GACGTGGC	2.65 (5%)	–	2.69 (5%)	2.33 (5%)
GATGAYRTGG	2.43 (3%)	–	2.30 (3%)	–
GCCACGTN	3.42 (4%)	–	3.74 (5%)	2.63 (3%)
CCACGTCA	2.50 (7%)	–	2.33 (7%)	2.15 (6%)
CCACGTCATC	3.39 (2%)	–	–	2.58 (2%)
E2F				
TYTCCCGCC	3.06 (3%)	–	–	2.06 (2%)
NCCCGCCA	7.80 (3%)	–	–	4.51 (2%)
GCGGGAAN	6.87 (4%)	–	–	3.91 (3%)
GGCGNNAA	2.83 (7%)	–	–	2.05 (5%)

up-regulated (Fig. 7); SIG4 regulates transcription of the plastid-encoded NDH-like complex gene *ndhF*.

Cis-Regulatory Elements Shared by FL-Responsive Cyclic Genes

We then asked whether these light/dark cyclic genes, whose expression was changing in concert during the FL treatment, shared conserved DNA sequence motifs in promoter regions. Cis-element analysis was performed by using ATCOECIS (Vandepoele et al., 2009). The consensus sequences identified in the promoter regions of these genes were identical with, or very similar to, common plant cis-elements (Table 1): I box (TCTTATC, complementary to GATAAGA), G box (CACGTG), and Z box (ATACGTGT) associated with light response, photosynthesis, and circadian regulation; ACGT-containing hexamer (Hex; ACGTCA) and the complementary TGA box (TGACGT), and E2F motifs (TTTCCCGC and the complementary GCGGGAAA) involved in the regulation of cell cycle and DNA replication. While these motifs typically appear in gene coexpression analysis (Vandepoele et al., 2009), their enrichment patterns differed between our samples. The promoter regions of the DE light/dark cyclic genes in all samples were enriched in I box-like CTTATCC; MO in two G box variants (CACGTGGC and CACGTGTA); Young leaves in a Z box-like TACGTGGA; and Young-MO and Mature-EOD in E2F-like motifs. The Hex and TGA box were overrepresented in all but Young-EOD (Table 1). The distinct motif enrichment patterns found in the four samples add further support to the interactions between FL, leaf development stage, and time of day in acclimatory regulation of gene expression.

DISCUSSION

FL Up-Regulates Genes for Protection against EL and Photooxidative Stress

Under fluctuating irradiance, light reactions in thylakoids respond almost instantaneously while the rate of CO_2 fixation changes more slowly, limited by the activation state of enzymes, the availability of CBC intermediates and ATP, or the slow response of stomata (Pearcy, 1990; Kaiser et al., 2018b; Slattery et al., 2018). When the light intensity drops from HL to LL, assimilatory charge (Laisk et al., 1984), which may be built up in C_3 plants under HL, continues to fuel the CBC in LL, resulting in a somewhat delayed decline of CO_2 uptake. Conversely, the slow response of CO_2 fixation upon LL-to-HL transition leads to EL absorption and excess e^- that can be transferred to oxygen to form $^1O_2$ and superoxide, respectively. Down-regulating PSII and linear e^- transport on the

one hand and scavenging excess e^- and ROS on the other hand are essential to mitigate photooxidative damage in such conditions.

Leaves of rainforest understory plants rapidly induce NPQ and accumulate zeaxanthin during sunflecks (Logan et al., 1997; Watling et al., 1997b). In the long term, frequent sunfleck exposure leads to pool size enlargement of the xanthophyll cycle pigments (Logan et al., 1997). Likewise, FL regimes, which are similar to the FL condition in this study, enhance photoprotective capacities in Arabidopsis leaves, as manifested by a parallel increase in the maximal NPQ, the pool size of the xanthophyll cycle pigments, and PSBS protein content (Alter et al., 2012; Caliandro et al., 2013). In Young and Mature leaves of this study, *PSBS*, *BCH1*, and *BCH2* were up-regulated (Figs. 7 and 8), which can positively affect NPQ and the xanthophyll cycle pool size (Davison et al., 2002; Li et al., 2002). In addition, Mature-EOD had increased gene expression of *ZEP* and *VDE* (Fig. 7). It has been reported that tobacco (*Nicotiana tabacum*) plants co-overexpressing *PSBS*, *ZEP*, and *VDE* achieved higher CO_2 assimilation under FL and ~15% more dry matter production in the field than the wild type (Kromdijk et al., 2016). The improved performance of the transgenic plants was ascribed to their ability to quickly adjust the levels of zeaxanthin and NPQ under FL (Kromdijk et al., 2016), since slow NPQ relaxation following HL-to-LL transition is predicted to cause losses in carbon gain (Zhu et al., 2004). Rapid NPQ relaxation may also be facilitated by the thylakoid H^+/K^+ antiporter KEA3 (Fig. 7), which releases H^+ from the lumen and thereby dissipates ΔpH to deactivate PSBS and VDE (thus NPQ) while increasing the contribution of the electric component of proton motive force for ATP synthesis (Armbruster et al., 2014, 2016). Concomitant up-regulation of these genes (Figs. 5 and 7) is in accordance with the necessity for efficient NPQ regulation under FL.

Notably, our results revealed increased gene expression of both NDH- and PGR5-dependent CEF pathway components under FL, especially in Mature leaves (Fig. 7). The PGR5-dependent CEF protects PSI against excess e^- by alleviating the acceptor side limitation and contributing to ΔpH formation, which then down-regulates e^- transport at PSII and Cyt b_6f (Munekage et al., 2002; Kono and Terashima, 2016; Suorsa et al., 2016). The ability to thus adjust e^- flows is critical in fluctuating conditions, as demonstrated by PSI photoinhibition and ultimate death of the *pgr5* mutant under FL (Munekage et al., 2002; Suorsa et al., 2012, 2016; Kono and Terashima, 2016). In comparison, NDH mutants (*crr4-3* and *ndho*) show only mild symptoms, and their growth is hardly affected in CL or FL (Suorsa et al., 2012, 2016). Hence, the contribution of the NDH-dependent CEF is considered minor in C_3 plants under FL (Kono et al., 2014; Kono and Terashima, 2016; Suorsa et al., 2016). Nevertheless, the marked co-up-regulation of *SIG4* (Supplemental Fig. S7) and NDH-like complex genes in Mature-EOD (Fig. 7), including all genes of nucleus-encoded subunits and protein factors except NDHS (or CRR31), argues for a role of this complex in FL acclimation. Photooxidative stress and H_2O_2 were shown to induce transcription of plastid-encoded NDH complex genes in barley (*Hordeum vulgare*) leaves (Martín et al., 1996; Casano et al., 2001). Also, increased NDH-dependent CEF was measured in Arabidopsis mutants (Strand et al., 2015), which produce high levels of H_2O_2 in leaves due to chloroplast FBPASE deficiency (*hcef1*; Livingston et al., 2010) or ectopic expression of photorespiratory GOX1 in chloroplasts (Fahnenstich et al., 2008). Accordingly, differential regulation of two CEF pathways has been proposed: the PGR5-dependent pathway regulated by redox change and the NDH-dependent pathway responding to H_2O_2 accumulation (Strand et al., 2016). The results of this study support the engagement of both pathways in long-term acclimation to the FL condition.

The ectopically expressed GOX1 oxidizes glycolate to glyoxylate in the light and thereby produces H_2O_2 in chloroplasts (Fahnenstich et al., 2008). As a result, the mutants develop small rosettes with patchy pale-green leaves under photorespiratory LL conditions and bleach under HL. Yet, this pale-green phenotype disappears when the mutants are grown under FL (Matsubara et al., 2016), suggesting an interplay between FL acclimation and H_2O_2 scavenging and/or signaling. Reinforcement of H_2O_2 detoxification under FL, as indicated by the up-regulation of *GPX7* and *CAT2* (Fig. 5; Supplemental Fig. S6) and the larger pool of ascorbate (Supplemental Table S1), may help the mutants keep H_2O_2 under control.

The expression of *GPX7* can be induced by HL, UV, and blue light via transcription factors HY5 and HYH downstream of photoreceptors UVR8 (UV-B-RESISTANCE8) and CRY1 (Kleine et al., 2007; Lee et al., 2007; Brown and Jenkins, 2008). These light signaling pathways also affect the expression of other stress-responsive genes we found in FL, such as *ELIPs*, *LHCB7*, *SIG5*, and *PDX* (Kleine et al., 2007; Brown and Jenkins, 2008; Onda et al., 2008). The up-regulation of *HYH* and *BIC1* (Fig. 5) may imply a role of blue light in acclimation to the FL condition. In fact, the Arabidopsis *cry1* mutant is sensitive to HL (Kleine et al., 2007), and a role of CRY1 in *LHCB* down-regulation (Ruckle et al., 2007) and $^1O_2$-dependent programmed cell death (Danon et al., 2006) has been proposed. The mechanisms by which CRY1 controls acclimation to EL and photooxidative stress are not yet understood.

Why Do Plants Up-Regulate CBC and Photorespiratory Genes under FL?

Given that limitation to CO_2 assimilation exacerbates EL and ROS production, photooxidative stress could be alleviated by removing limitations in the CBC. The up-regulation of CBC genes under FL (Fig. 7) is in line with this notion. Of the three genes (*CP12-2*, *FBA1*, and *SBPASE*) that were up-regulated in all FL samples

(Fig. 5), *FBA*, *SBPASE*, or both, when overexpressed, have been shown to increase CO_2 assimilation in tobacco and Arabidopsis leaves, consistent with the control of these enzymes over the CBC activity (Lefebvre et al., 2005; Uematsu et al., 2012; Simkin et al., 2015, 2017). Despite the up-regulation of these genes, however, Young and Mature leaves had lower ETR (Fig. 2B) and less Suc and starch under FL (Fig. 3, A and B). Furthermore, the maximal rates of RuBP regeneration and Rubisco carboxylation were unchanged in Mature leaves after 3 d under FL (Fig. 2D). This agrees with the report that nongrowing mature leaves of Col-0 plants did not up-regulate the CO_2 fixation capacity during long-term acclimation to HL (Athanasiou et al., 2010), whereas leaves grown in HL do (Vialet-Chabrand et al., 2017). Importantly, leaves of Col-0 did not increase the CO_2 fixation capacity when grown under FL conditions (Vialet-Chabrand et al., 2017), suggesting limited efficacy of FL to trigger acclimatory enhancement of CO_2 assimilation. The previous studies in rainforest species also provided little or no evidence for enhancement of the area-based photosynthetic capacity in plants grown under FL (Watling et al., 1997a; Leakey et al., 2002). The discrepancy between the responses of CBC gene expression (Fig. 7) and CO_2 fixation (Fig. 2D) found in Mature leaves after 3 d in the FL condition may be explained by translational or posttranslational regulation (Kawaguchi et al., 2004; Schürmann and Buchanan, 2008; Zaffagnini et al., 2012; Pal et al., 2013; Oelze et al., 2014; Geigenberger et al., 2017). It is also possible that the maximum photosynthesis rate, which is measured at steady state, is not a good indicator of FL acclimation. Under FL, plants may adjust other traits, such as enzyme activation (Yamori et al., 2012) or energy storage during transient HL (Laisk et al., 1984).

While up-regulation of photosynthetic genes was more pronounced in Mature leaves, the expression of photorespiratory genes was similarly up-regulated in both Young and Mature leaves (Fig. 7). Photorespiration protects photosynthesis against photoinhibition by recycling the carbon of glycollate-2-phosphate and by serving as a sink for ATP and reduced FD (Osmond and Grace, 1995; Wingler et al., 2000; Takahashi et al., 2007). In addition, Gly, which is synthesized in the photorespiratory pathway, supports glutathione accumulation in leaves (Noctor et al., 1999). The balance between RuBP carboxylation and oxygenation shifts toward the latter as [CO_2] in the chloroplast stroma declines. Since stomatal conductance responds much more slowly than photochemical and biochemical reactions of photosynthesis upon LL-to-HL transition, the [CO_2] inside the leaf transiently drops under FL conditions (Vialet-Chabrand et al., 2017) to promote photorespiration (Huang et al., 2015). Parallel up-regulation of photorespiratory genes along with *BCA1* and *BCA4* (Fig. 7) is in agreement with increased photorespiration under FL.

Leaves grown under FL had lower levels of Gly, Ser, and glyoxylate (Supplemental Fig. S1; Supplemental Table S1), three photorespiratory metabolites that are implicated in feedback regulation of photorespiratory gene expression and RuBP supply (Wingler et al., 2000; Timm et al., 2016). Only glycerate, which inhibits SBPASE and FBPASE in the RuBP regeneration phase of the CBC (Schimkat et al., 1990), showed 40% or 70% increase under FL (Supplemental Table S1). The regulation of SBPASE and FBPASE activities by redox and glycerate (Schimkat et al., 1990; Schürmann and Buchanan, 2008), along with ROS-induced modifications of redox-regulated CBC enzymes (Zaffagnini et al., 2012), may attune metabolic flux in the CBC and photorespiratory pathway under photooxidative FL conditions.

FL Alters Gene Expression in Pigment and Prenylquinone Metabolism

Consistent with the decline in *LHCB* gene expression (Fig. 7; Supplemental Fig. S6, A and B) and Chl content during long-term FL exposure (Alter et al., 2012; Caliandro et al., 2013), we found down-regulation of *PORA* and *PORB* and up-regulation of Chl breakdown genes (Fig. 8). Phytol is released during Chl degradation to be recycled as the side chain of tocopherols or esterified to fatty acids in plastoglobuli (Ischebeck et al., 2006; Lippold et al., 2012; vom Dorp et al., 2015). Mature leaves grown under FL showed 70% or 170% increase in phytol on day 7 (Supplemental Table S1), and both Young and Mature leaves showed up-regulation of tocopherol biosynthetic genes on day 3 (Fig. 8), albeit not *VTE5* and *VTE6* encoding phytol kinase and phytyl-phosphate kinase, which mediate the phytol recycling (Valentin et al., 2006; vom Dorp et al., 2015). The parallel up-regulation of genes involved in Chl breakdown, prenylquinone and carotenoid biosynthesis, as well as *ABC1Ks* (Figs. 5 and 8) is indicative of increased metabolism and exchange of pigments and prenyllipids in thylakoids and plastoglobuli under FL.

Mature leaves of the FL plants also accumulated greater amounts of polyunsaturated fatty acids at EOD (Supplemental Table S1), and all FL samples had increased transcript levels of *FAD8* and *FAD4* (Fig. 5) for synthesis of 18:3 ω-3 and trans-16:1, especially for PG (Román et al., 2015). Unsaturated fatty acids are prone to peroxidation by ROS. In the lipid bilayer or bound to photosynthetic protein complexes, some unsaturated fatty acids may be oxidized in the FL condition. Tightly bound PG molecules are found in both PSI and PSII cores (Umena et al., 2011; Mazor et al., 2017) and in the monomer-monomer interface of LHCII trimers (Liu et al., 2004). Bound in these complexes are also Chls and carotenoids. Continuous turnover of Chl *a* and β-carotene, presumably as part of the PSII D1 repair cycle (Baena-González and Aro, 2002), has been reported in Arabidopsis leaves (Beisel et al., 2010, 2011). The increased expression of Chl and carotenoid biosynthetic genes in Mature leaves (Fig. 8), despite the decline in *LHCB* expression and Chl content, may reflect high turnover of these pigments in photooxidative FL conditions. It is noteworthy that *PORC*, the only

POR gene that was up-regulated in Mature-EOD under FL (Fig. 8), is HL inducible, and seedlings of a PORC-deficient Arabidopsis mutant accumulate less than 50% of the wild-type Chl level when grown in HL (Masuda et al., 2003). The contrasting FL responses of three *POR* genes suggest separate regulation of Chl biosynthesis for light harvesting and damage repair.

Compared with the pathways of Chl catabolism and recycling, much less is known about the fate of carotenoids. Oxidation of carotenoids produces various apocarotenoids, including reactive electrophile species (e.g. β-cyclocitral), which react with redox-active compounds, especially thiols, to affect redox signaling and gene transcription (Ramel et al., 2012; Havaux, 2014). Although contributions of nonenzymatic and enzymatic carotenoid cleavage are not yet clarified in leaves, our FL samples showed up-regulation of *CCD1* and *CCD4* (Fig. 8). Cleavage by CCD4 is specific to the 9,10 (9′,10′) double bond of cyclic all-trans-carotenoids and apocarotenoids (Lätari et al., 2015; Bruno et al., 2016). All photosynthetic carotenoids, except 9′-cis-neoxanthin, are potential substrates of CCD4. The cytosolic CCD1 (Auldridge et al., 2006) may then remove oxidation products (nonenzymatic or enzymatic) of carotenoids, since it can cleave a range of cyclic and acyclic carotenoids and apocarotenoids at different positions of the double bond (Schmidt et al., 2006; Vogel et al., 2008). During leaf senescence, β-carotene, lutein, and violaxanthin are retained (Biswal, 1995) or cleaved by CCD4 (Rottet et al., 2016) in plastoglobuli. Also in non-senescent leaves, CCD4-dependent cleavage of all-trans-xanthophylls has been detected (Lätari et al., 2015). To what extent pigment and lipid turnover contributes to maintenance and acclimation of thylakoids is a question worth investigating in the future.

How Is Global Reprograming of Gene Expression Coordinated during FL Acclimation?

The persistent oscillation of DE cyclic genes following the transfer from CL to FL (Supplemental Fig. S6) demonstrates a fundamental role of diel programs in organizing acclimatory adjustment of gene expression in leaves. Circadian regulation of gene expression is integral to plant stress responses, such as low temperature, UV-B, ROS, and pathogens (Dong et al., 2011; Fehér et al., 2011; Wang et al., 2011; Lai et al., 2012; Takeuchi et al., 2014). Due to rhythmic gene expression in leaves, observations based on a single time point may be biased toward genes and responses that are gated at that specific time of day (Bieniawska et al., 2008). The small overlaps found between our DE genes in MO and at EOD (Fig. 4B) underline the necessity to study the gene expression response at multiple times of day.

The plant circadian clock orchestrates gene transcription and synchronizes biological processes with recurring changes in environments (Farré, 2012; Hsu and Harmer, 2014; Greenham and McClung, 2015). Coexpression of photosynthetic genes from morning to midday is a well-known example of clock regulation operating at the transcriptional level (Harmer et al., 2000). The contrasting but coordinated FL responses of morning and evening genes, as found in Figure 9, invite a question about coadjustment mechanisms of cyclic gene expression during acclimation. The overrepresentation of G and Z box-like motifs in the promoter regions of the DE light/dark cyclic genes in MO (Table 1) corresponds to the enrichment of light stimuli and chloroplast components in the DE genes (Supplemental Tables S2 and S3). The role of these motifs is well established for light-dependent regulation of *RBCS* and *LHCB* promoters in combination with I box or I box-like GATA element (Argüello-Astorga and Herrera-Estrella, 1998). A large number of G and Z box elements are targeted by HY5 and PHYTOCHROME INTERACTING FACTOR3 downstream of phytochromes, CRYs, and UVR8 during photomorphogenesis and UV-B response (Yadav et al., 2002; Jiao et al., 2007). In principle, FL could modulate light-responsive gene transcription via photoreceptors. We note, however, that our list of DE genes includes only a small fraction of genes having a G or Z box.

Combinatorial or competitive binding of multiple transcription factors in neighboring DNA regions confers context-dependent complex regulation of gene transcription. In the case of *LHCB1* promoters, for instance, binding of the clock oscillator CCA1 to CCA1-binding sites enhances adjacent G box binding of HY5, and this interaction is modulated by phosphorylation of CCA1 and HY5 (Hardtke et al., 2000; Andronis et al., 2008). Genes regulated by a G box typically exhibit light/dark cyclic expression (Ezer et al., 2017), and conversely, the G box motif is enriched in target DNA-binding regions of clock components, CCA1, TOC1, PRR5, PRR7, and PRR9 (Gendron et al., 2012; Huang et al., 2012; Nakamichi et al., 2012; Liu et al., 2013, 2016; Nagel et al., 2015), most of which were up-regulated in the FL condition (Supplemental Fig. S7). Combinatorial interplay is also well known for ABA-inducible gene promoters having G box-like ACGTGGC together with coupling elements (Shen and Ho, 1995) or auxin-inducible soybean (*Glycine max*) *GH3* promoter having Hex/TGA boxes next to auxin-responsive elements (Ulmasov et al., 1995). The TGA box TGACGT and Hex CCACGTCA are similar (or complementary) to the stress-induced unfolded protein response (UPR) element TGACGTGR (R is for A or G) found in animal and plant UPR genes (Martínez and Chrispeels, 2003; Oh et al., 2003). In this study, the Hex/TGA box motifs were overrepresented in the DE cyclic genes in MO and Mature-EOD, whereas the canonical G box was enriched only in MO (Table 1). This might imply that, during FL acclimation, light signals predominantly act in MO, while Hex/TGA-related signals impinge both in MO and at EOD. Circadian gating of light signal transduction offers another possible explanation for the overrepresentation of the G box in the DE morning genes.

The results in Figure 9 and Table 1 also pointed to parallel down-regulation of cell cycle-related evening

genes having E2F motifs. The retinoblastoma/E2F pathway controls cell cycle and DNA replication in mammalian and plant cells (Stals and Inzé, 2001; Trimarchi and Lees, 2002). The activation of E2F/DP transcription factors, which control the entry to DNA replication phase, is regulated by growth and stress signals such as sugars and hormones (Stals and Inzé, 2001). Changes in these signals could alter the expression of E2F motif-containing cell cycle genes. Diel variations of starch and hormone levels (Bläsing et al., 2005; Nováková et al., 2005), supported by circadian regulation of transcription in these pathways (Harmer et al., 2000; Smith et al., 2004; Covington et al., 2008; Michael et al., 2008a), may underlie cyclic expression of cell cycle genes in leaves. Interestingly, Young leaves down-regulated E2F motif-containing evening genes in MO (Fig. 9, B and C; Table 1), when hypocotyl growth exhibits a circadian peak in Arabidopsis (Nozue et al., 2007). In contrast, down-regulation in Mature leaves was more pronounced at EOD, when the expression of these genes reaches the maximum in light/dark conditions (Fig. 9, B and C). Since cell proliferation ceases at an early stage of leaf development in Arabidopsis (Andriankaja et al., 2012), the repression of cell cycle genes found in Young and Mature leaves under the FL condition may reflect endoreduplication rather than cell division.

FL Induces SAR-Like Gene Expression in Young Leaves

Alongside the time of day-dependent adjustments of gene expression, our results draw attention to the distinct gene expression responses in Young and Mature leaves, especially at EOD (Fig. 4). Young leaves synthesize cell components as they grow, whereas Mature leaves mostly do maintenance in unchanging conditions. In addition, long-term acclimation involves biochemical and morphological alterations in Young leaves, whereas Mature leaves must rely on the former. Despite the similar phenotypic alterations found for PSII (Fig. 2, A–C) and metabolites (Fig. 3; Supplemental Fig. S1), these leaves differ in acclimatory reprogramming of gene expression.

Unexpectedly, we found FL-induced up-regulation of SAR-like genes in Young leaves (Fig. 6; Supplemental Fig. S4, A and B), which also had higher SA contents than Mature leaves (Supplemental Fig. S5, A and B). While FL did not enhance SA accumulation, it tended to increase Pip (Supplemental Fig. S5C), even though the increase was rather small compared with the levels seen after pathogen inoculation (Návarová et al., 2012). The specific patterns of SAR-like gene expression found in Young leaves under FL (Fig. 6) might be explained by concerted actions of Pip and SA (Bernsdorff et al., 2016). The SA-dependent *PR* gene induction is mediated by NPR1 (NONEXPRESSOR OF PR GENES1), which moves from the cytoplasm to the nucleus in a redox-dependent manner (Mou et al., 2003). In the nucleus, NPR1 forms a complex with TGA box-binding factors (Johnson et al., 2003; Zhang et al., 2003). This pathway is constitutively active in the *cpr5* mutant, which accumulates large amounts of SA (Bowling et al., 1997). Whether the FL-induced SAR-like gene expression engages the NPR1-dependent pathway is not known.

Marked SA accumulation has been reported in the *ceh1* (*constitutively expressing hydroperoxide lyase1*) mutant, which exhibits up-regulation of *ICS1* and other stress-responsive genes, such as marker genes of SA, JA, and UPR (Xiao et al., 2012; Walley et al., 2015; Lemos et al., 2016). The mutation in *ceh1* causes amino acid substitution in the MEP pathway enzyme 1-hydroxy-2-*C*-methyl-2-(*E*)-butenyl-4-diphosphate synthase, resulting in accumulation of its substrate MEcPP. Increased accumulation of MEcPP has been detected in Arabidopsis leaves under HL or upon wounding, which was accompanied by transcriptional activation of stress-responsive genes (Xiao et al., 2012). Similarly, the reactive electrophile species β-cyclocitral was shown to up-regulate *ICS1* to enhance SA accumulation (Lv et al., 2015). Unlike *ceh1* and β-cyclocitral treatment, however, our FL condition neither up-regulated these genes nor increased SA in leaves (Supplemental Fig. S5A). Thus, the up-regulation of SAR-like genes found in Young leaves (Fig. 6; Supplemental Fig. S4), but not in Mature leaves, is distinct from the stress responses triggered by MEcPP and β-cyclocitral. The differences may be partly explained by the mild effects of our FL treatment, which did not cause severe stress symptoms.

CONCLUSION

Acclimation to photooxidative FL conditions encompasses global reprogramming of gene expression in Arabidopsis leaves, including genes for photoprotection, photosynthesis, and photorespiration as well as pigment, prenylquinone, and vitamin metabolism. Since many genes undergo day/night cyclic expression in leaves, long-term large-scale adjustment of gene expression proceeds in the temporal framework defined by diel and circadian programs. To identify acclimatory gene modules and understand their regulatory networks, also in combination with different abiotic and biotic stress factors, remains a key research target to develop strategies for improving plant performance in changing environments.

MATERIALS AND METHODS

Plant Materials and Growth Conditions

Seeds of Arabidopsis (*Arabidopsis thaliana*) Col-0 were sown on moist soil (type Pikier; Balster Einheitserdewerk) and stratified at 5°C in the dark for 4 d before being transferred to the climate chamber. The initial growth condition in the climate chamber was a 12-h/12-h light/dark cycle with 23°C/18°C air temperature at 60% relative air humidity. The intensity of photosynthetically active radiation provided by fluorescent tubes (Fluora L36 W/77; Osram) was ~75 μmol photons m^{-2} s^{-1} (CL). After 2 weeks, seedlings were transferred to pots (7 × 7 × 8 cm, one plant per pot) filled with soil (type ED 73; Balster Einheitserdewerk). After 2 or 3 more weeks of cultivation in the CL condition,

plants were divided into two groups. One group was kept in CL while the other group was transferred to an FL condition in which 20-s pulses of ~1,000 μmol photons m^{-2} s^{-1} were applied by a white LED (IP65; as-Schwabe) moving over the plants every 5 min under the CL condition during the light period. The duration and frequency of FL were controlled by the computer program as described previously (Alter et al., 2012). Although the application of HL pulses increased the average light intensity (~137 μmol photons m^{-2} s^{-1}) under FL, acclimatory responses of LL-grown Arabidopsis plants are essentially the same regardless of whether HL pulses do or do not increase the average light intensity under FL (Alter et al., 2012).

Chl Fluorescence Analysis

Chl fluorescence measurements were performed with Imaging-PAM MAXI (Heinz Walz) at the end of the dark period on day 3. An area of interest was selected inside Young and Mature leaves of three replicate plants (per condition) by avoiding the leaf margin. After measuring the F_v/F_m, actinic light was applied by the blue LED of MAXI-PAM to obtain rapid light response curves of ETR and NPQ. Light intensity was increased stepwise from 0 to ~1,075 μmol photons m^{-2} s^{-1} with a dwell time of 20 s at each step. The Chl fluorescence parameters were calculated as $F_v/F_m = (F_m - F_0)/F_m$, $NPQ = (F_m - F'_m)/F'_m$, and ETR = photosynthetically active radiation $\times$ 0.84 $\times$ 0.5 $\times$ $(F'_m - F)/F'_m$, where F_m and F_0 are the maximal and minimal fluorescence intensity of dark-adapted leaves and F'_m and F are the maximal and actual fluorescence intensity of illuminated leaves.

Gas-Exchange Measurements

CO_2-exchange rates were measured in mature leaves of five replicate plants (per condition) on the morning of day 3 using an LI-6400XT with a red and blue LED light source (LI-COR). Measurements were performed in the climate chamber in which the CL and FL plants were growing (air temperature 23°C and relative humidity 60%). The intensity of the LED was set to 800 μmol photons m^{-2} s^{-1}. Leaves were allowed to reach steady state under this light intensity and 400 μL L^{-1} CO_2, which took 20 to 30 min. During this initial stabilization, leaf temperature increased to 26°C or 26.5°C but did not change further until the end of the measurement. The CO_2 concentration inside the measuring cuvette was adjusted stepwise with a dwell time of 4 to 5 min at each step (400, 250, 150, 100, 50, 400, 550, 700, 900, 1,100, 1,300, and 1,500 μL L^{-1}). The A/C_i curves were analyzed according to Sharkey et al. (2007) to estimate the J_{max} and V_{cmax}.

Growth Analyses

Leaf growth analysis was started at the onset of the FL and CL treatment (day 0). Projected rosette leaf area (Fig. 1B) was determined for each of the 45 and 42 plants of the FL and CL treatments, respectively, by using the GROWSCREEN-FLUORO method (Jansen et al., 2009). Measurements were repeated daily at around ZT4, when leaves were in almost horizontal positions. The mean relative growth rate (% d^{-1}) during the experiment was calculated by fitting growth curves to an exponential function and multiplying the growth factor by 100.

The aboveground part of 17 and 20 plants (for the FL and CL conditions, respectively) was harvested at the end of the experiment (day 7) to measure fresh and dry weights. Fresh weight was measured using an analytical balance (XS205 DualRange; Mettler-Toledo) immediately after excision. Dry weight was determined after drying at 70°C until a constant mass was reached. Leaf mass per area was then calculated for each plant based on the dry weight and the projected rosette leaf area measured on day 7.

Pigment Analysis

Leaf discs (56 mm^2 from Young leaves and 100 mm^2 from Mature leaves) were taken from four replicate plants (per condition) in MO of day 3 under the FL and CL conditions, immediately frozen in liquid N_2, and stored at −80°C until extraction. Photosynthetic pigments were extracted by grinding frozen leaf discs in 1 mL of acetone. The homogenate was centrifuged at 13,000 rpm for 5 min, and the supernatant was filtered (0.45-μm True Syringe Filter; Alltech Associates) before an aliquot (20 μL) was injected into an HPLC system. Chls and carotenoids were separated on an Allsphere ODS-1 column (5 μm; Alltech Associates) by using the method described by Matsubara et al. (2005). Photosynthetic pigments were identified based on retention times and absorption spectra recorded by a Waters 996 photodiode array detector. Peak areas were integrated at 440 nm (Chl *a* and carotenoids) or 470 nm (Chl *b*) with Waters Empower software to determine Chl contents per unit of leaf area and levels of individual carotenoids relative to the total Chl.

Measurements of Suc and Starch

Young and Mature leaves were harvested from four replicate plants (per time point and per condition) in MO and at EOD of day 3 under the FL and CL conditions. After measuring the fresh weight with an analytical balance (XS205 DualRange; Mettler-Toledo), leaves were shock frozen in liquid N_2 and stored at −80°C until extraction. Leaves were homogenized by using TissueLyser II (Qiagen). Soluble sugars were extracted twice with 400 μL of 80% (v/v) ethanol in 2 mM HEPES followed by twice with 400 μL of 50% (v/v) ethanol in 2 mM HEPES, incubating each time for 15 min at 80°C. Soluble sugar contents were determined by coupled enzymatic assay (Jones et al., 1977). Glc-6-P dehydrogenase, Glc-6-P isomerase, and hexokinase were purchased from Roche Diagnostics and invertase from Carl Roth. Absorption changes at 340 nm, arising from the reduction of $NADP^+$ to NADPH, were measured with a Synergy 2 microplate reader (BioTek).

The pellets from sugar extraction were resuspended in 500 μL of water before autoclaving at 120°C and 0.1 MPa for 90 min. Starch was digested enzymatically using α-amylase and amyloglucosidase (Roche Diagnostics). An aliquot (100 μL) was taken from each sample, mixed with 400 μL of 50 mM sodium acetate buffer (pH 4.9) containing the enzymes, and incubated at 37°C for 16 h for starch digestion. Subsequently, soluble sugar (Glc) was measured as described above.

Determination of Amino Acids and Pip

Young and Mature leaves were harvested in MO and at EOD of day 3 under the FL and CL conditions, frozen in liquid N_2, and stored at −80°C until extraction. Twelve leaves from six plants were pooled together for each of the three or four biological replicates for analyses of amino acids and defense hormones (Pip, SA, SA glucosides, and JA). Free amino acids were extracted from 60 mg of homogenized frozen leaf material in 500 μL of 25% acetonitrile in 0.01 M HCl. After adding 10 μL of heptylamine (2 mg mL^{-1}), the samples were mixed thoroughly for 15 min at room temperature and centrifuged at 14,000 rpm for 4 min. The supernatant (100 μL) was taken, and amino acids were extracted with the EZ:faast free amino acid analysis kit for gas chromatography-mass spectrometry (GC-MS; Phenomenex) as specified in the manufacturer's instructions. Subsequently, the samples were dissolved in 70 μL of dichloromethane, and 3 μL was injected into the GC-MS apparatus (GC 7890A; Agilent Technologies). Amino acids were separated on a silica capillary column (ZB-AAA, 10 m $\times$ 0.25 mm; Phenomenex). The GC-MS measurements and amino acid quantification were performed as described by Návarová et al. (2012). The method did not allow determination of Arg and Met.

Analysis of SA, SA Glucosides, and JA

For the analysis of SA, SA glucosides, and JA, 150 mg of the homogenized frozen leaf material was taken from the samples described for amino acid analysis. After adding 600 μL of preheated (70°C) extraction buffer (water:1-propanol:HCl, 1:2:0.005), a mixture of D_4-SA and dihydro-JA (3.33 ng μL^{-1} each) was added to each sample as an internal standard. The samples were then mixed with 2 mL of dichloromethane, and organic supernatants were separated for the analysis of SA and JA, while pellets and inorganic supernatants were collected for the extraction of SA glucosides. Water was removed from the organic supernatants by using Na_2SO_4. To remove solvent, vapor-phase extraction was conducted with Porapak-Q absorbent (VCT-1/4X3-POR-Q; Analytical Research Systems). Metabolites were eluted from the collector trap with dichloromethane, and the sample volume was reduced to 30 μL before storage at −20°C.

For extraction of SA glucosides, 1 mL of 0.1 M HCl was added to the pellets and inorganic supernatants before mixing with 30 μL of the internal standard and heating to 100°C for 30 min. After cooling, dichloromethane (2 mL) was added and organic and inorganic phases were separated. The organic phase was dried three times with Na_2SO_4, and solvent was evaporated under an N_2 gas stream. The extracts were methylated with dichloromethane (300 μL) and methanol (60 μL). The vapor-phase extraction was performed as described above.

The sample mixture (4 μL) was injected into the GC-MS apparatus (GC 7890A; Agilent Technologies) and separated on a fused silica capillary column (ZB-5MS, 30 m × 0.25 mm; Zebron, Phenomenex). The separation was performed as described by Mishina and Zeier (2006). The mass spectra were recorded with a combined 5975C MS detector (Agilent Technologies) in the electron ionization mode. Peak areas of ion chromatograms were integrated for typical ions of the metabolites by using Agilent software.

Metabolic Profiling

For each of the six replicate samples (per time point and per condition), Mature leaves (~500 mg) were harvested from six or seven plants on day 7, pooled together, and immediately frozen in liquid N_2. The frozen leaf samples were sent to Metabolomic Discoveries for nontargeted profiling of metabolites. The methods of sample extraction and derivatization, instrument settings, and data analysis are as described by Lisec et al. (2006). The concentrations of metabolites were normalized to the internal standards, and data were tested for normality (Shapiro-Wilk test) and variance homogeneity (F test) using the appropriate statistical tests (Student's t test, Welch test, and Mann-Whitney test). Relative changes in the FL samples compared with the corresponding CL samples were then calculated for each metabolite. The changes were considered significant at $P < 0.05$. Statistical analyses were performed using the software JMP Genomics 5.1 (SAS Institute).

RNA-Seq Analysis

Young and Mature leaves were collected from three replicate plants (per time point and per condition) on day 3. Leaves were immediately frozen in liquid N_2 and stored at −80°C until RNA extraction. Total RNA was isolated by using the RNeasy Plant Mini kit (Qiagen) according to the manufacturer's instructions. The RNA quality was checked in aliquots by running denaturing agarose gels. Additional aliquots were taken and kept for RT-qPCR validation of RNA-Seq results. The remaining total RNA extracts were frozen in liquid N_2 and sent to the Genomics Core Facilities of the EMBL for sequencing (Illumina HiSeq 2000; 50-bp paired-end reads). The complementary DNA (cDNA) library was prepared from each RNA sample (i.e. each biological replicate) and individually barcoded. Then all samples were pooled together and sequenced six times using three different sequencing lanes (i.e. two technical repetitions per lane) to account for within-lane and between-lanes variability.

The initial quality check of RNA-Seq reads was performed using FastQC V0.10.1 (https://www.bioinformatics.babraham.ac.uk/projects/fastqc; Schmieder and Edwards, 2011). After reads were trimmed and technical sequences (adapters, PCR primers, or fragments thereof) were removed by Trimmomatic V0.30 (http://www.usadellab.org/cms/index.php?page=trimmomatic; Bolger et al., 2014), data quality was checked again by FastQC. The Burrows-Wheeler Alignment tool and BLAST were used for sequence alignment. Gene annotation was based on the gene function descriptions AGI Locus TAIR10 (August 2012) of TAIR (https://www.arabidopsis.org). For the DE genes shown in Figures 5, 7, and 8 and Supplemental Figure S4, annotation was updated manually using the TAIR Web site.

For each gene in each biological replicate, a mean value was calculated from the reads of six technical (sequencing) replicates. Differential gene expression was analyzed between three biological replicates of the FL samples and the CL samples by using edgeR V3.14.0 (Bioconductor; http://bioconductor.org; Robinson et al., 2010; McCarthy et al., 2012). Data were excluded from further analyses unless CPM > 3 and the differential expression was supported by FDR < 0.01. Overrepresentation of Gene Ontology (GO) cellular components and biological processes in the DE genes was analyzed using the PANTHER classification system (http://www.geneontology.org/page/go-enrichment-analysis; Mi et al., 2013).

RT-qPCR Analysis

For validation of RNA-Seq results, cDNA was synthesized from 1 μg of total RNA (aliquots of the total RNA samples used for RNA-Seq) with the iScript cDNA synthesis kit (Bio-Rad Laboratories) and diluted to 1:10 by water. The RT-qPCR reactions were performed with the iCycler iQ real-time PCR detection system (Bio-Rad) using iQ SYBR Green Supermix (Bio-Rad) and following the manufacturer's recommendations. Four genes (*LHCB1.2*, *ELIP2*, *GPX7*, and *PR2*) were analyzed to cover a wide range of fold change. The transcript abundance of the target genes was normalized to *LCYE* (*LYCOPENE EPSILON CYCLASE*), which served as an endogenous reference in each sample.

For analysis of DE cyclic genes (*LHCB1.2*, *CAT2*, *ELIP2*, *GPX7*, *CCA1*, and *ELF3*), Young and Mature leaves were harvested from three or four replicate plants (per time point and per condition) at seven time points (ZT23, ZT1, ZT3, ZT7, ZT11, ZT15, and ZT19) during the light/dark cycle of day 1 and day 3. Leaf samples were immediately frozen in liquid N_2 and lyophilized. Total RNA was isolated by using the E.Z.N.A. Plant RNA kit (Omega Bio-tek) followed by DNase treatment (Ambion TURBO DNA-*free* kit; Fisher Scientific). Then cDNA was prepared from 500 ng of total RNA using the iScript cDNA synthesis kit (Bio-Rad) and diluted to 1:5 by water. The RT-qPCR was performed with Mastercycler ep *realplex* 2 (Eppendorf) using Applied Biosystems SYBR Green PCR Master Mix (Thermo Fisher Scientific) according to the user guide. Two genes, *LCYE* and *ISOPENTENYL PYROPHOSPHATE:DIMETHYLALLYL PYROPHOSPHATE ISOPERASE2*, served as endogenous references for gene expression analysis. Supplemental Table S5 shows the sequences of all primers used in the RT-qPCR experiments.

Comparison with Public Arabidopsis Leaf Transcriptome Data

The expression patterns of highly up-regulated genes (FL/CL ≥ 4) were compared with public Arabidopsis microarray data sets studying biotic stress and hormone responses as described by Gruner et al. (2013). The following data sets were included in the comparison: systemic (nontreated) leaves of Col-0 2 d after inoculation with *Psm* inducing SAR versus mock (SAR 48 h), *cpr5* mutant versus Col (*cpr5*/Col), local (treated) leaves of Col-0 24 h after inoculation with *Psm* versus mock (*Psm* 24 h), Col versus SA-deficient or JA- and ethylene-insensitive mutants 24 h after inoculation with *Psm* (Col/*sid2*, Col/*coi1*, and Col/*ein2*), 2 h after spraying with 1 mM SA versus mock (SA 2 h), 3 h after treatment with 10 μM MeJA versus mock (MeJA 3 h), 1 h after application of 20 mM H_2O_2 versus mock (H_2O_2 1 h), 3 h after treatment with 10 μM ABA versus mock (ABA 3 h), 3 h after treatment with 1 μM IAA versus mock (IAA 3 h), and 4 h after treatment with 1 mM 22-mer peptide of the elicitor-active domain of bacterial flagellin versus mock (flg22 4 h). The sources of the public data sets are described by Gruner et al. (2013). The FiRe Excel macro program (Garcion et al., 2006) was used for data alignment.

Identification of Cyclic Genes

Cyclic genes were identified with the Web-based tool Phaser (http://phaser.mocklerlab.org; Mockler et al., 2007) by using our DE genes as queries. The cyclic gene data sets of Bläsing et al. (2005) in a 12-h/12-h light/dark condition and of Edwards et al. (2006) in a continuous light condition were used as reference for light/dark cyclic and circadian regulated genes, respectively. The correlation cutoff was set to 0.8. Biological processes of the DE cyclic genes were analyzed by MapMan version 3.5.1 (https://mapman.gabipd.org; Thimm et al., 2004).

Cis-Element Analysis

Putative cis-regulatory elements were searched in promoter regions of the DE cyclic genes using ATCOECIS (http://bioinformatics.psb.ugent.be/ATCOECIS; Vandepoele et al., 2009). The motif search was restricted to 1,000-bp upstream regions from the translation start site (or shorter if the adjacent gene is located within this region). We considered only those motifs that fulfilled the following four criteria: (1) the upstream regions were enriched in the motif by more than 2-fold compared with the genome-wide occurrence; (2) the enrichment is significant at $P < 0.01$; (3) the motif is shared by greater than 1% of the DE light/dark cyclic genes in the sample; and (4) the motif satisfies the above three criteria in more than one sample.

Statistical Analysis

For measurements of Chl fluorescence and growth as well as the contents of sugar, pigments, and hormones, data were statistically analyzed by Student's t test. For metabolomic and RNA-Seq analyses, the statistical methods used are described in the corresponding sections.

Accession Numbers

Gene sequence data from this article can be found in the TAIR database under the accession numbers listed in Supplemental Data (all DE genes). Raw RNA-Seq data (288 files for 144 data sets) are available at the European Nucleotide Archive (ENA) under the project ID PRJEB31094.

Supplemental Data

The following supplemental materials are available.

Supplemental Figure S1. Levels of free amino acids in leaves after a 3-d exposure to the FL or CL condition.

Supplemental Figure S2. Selection of fold change cutoff values for differential gene expression analysis between FL and CL.

Supplemental Figure S3. Validation of RNA-Seq fold change values by RT-qPCR.

Supplemental Figure S4. Heat maps of the responses of highly up-regulated genes to biological stress and hormone treatments.

Supplemental Figure S5. Accumulation of SA, SA glucosides, and Pip in leaves on day 3 under the FL and CL conditions.

Supplemental Figure S6. Cyclic gene expression in leaves on day 1 and day 3 under the FL and CL conditions.

Supplemental Figure S7. Differentially expressed cyclic genes associated with the circadian clock.

Supplemental Table S1. Fold changes of metabolites in Mature leaves on day 7.

Supplemental Table S2. Overrepresentation of GO cellular components associated with up- and down-regulated genes under FL.

Supplemental Table S3. Overrepresentation of GO biological processes associated with up- and down-regulated genes under FL.

Supplemental Table S4. List of highly up-regulated genes that were not included in Figure 6 and Supplemental Figure S4.

Supplemental Table S5. List of primers used for the RT-qPCR experiments.

Supplemental Data. Lists of DE genes under FL compared with CL.

ACKNOWLEDGMENTS

We thank Beate Uhlig and Marcel Schneider for their assistance during plant cultivation and Andreas Averesch and Kathrin Heinz for the maintenance of the moving LED system and GROWSCREEN-FLUORO, respectively.

Received November 20, 2018; accepted January 23, 2019; published February 4, 2019.

LITERATURE CITED

Alter P, Dreissen A, Luo FL, Matsubara S (2012) Acclimatory responses of *Arabidopsis* to fluctuating light environment: Comparison of different sunfleck regimes and accessions. Photosynth Res **113:** 221–237

Anderson JM, Chow WS, Goodchild DJ (1988) Thylakoid membrane organization in sun/shade acclimation. Aust J Plant Physiol **15:** 11–26

Andriankaja M, Dhondt S, De Bodt S, Vanhaeren H, Coppens F, De Milde L, Mühlenbock P, Skirycz A, Gonzalez N, Beemster GTS, et al (2012) Exit from proliferation during leaf development in *Arabidopsis thaliana*: A not-so-gradual process. Dev Cell **22:** 64–78

Andronis C, Barak S, Knowles SM, Sugano S, Tobin EM (2008) The clock protein CCA1 and the bZIP transcription factor HY5 physically interact to regulate gene expression in *Arabidopsis*. Mol Plant **1:** 58–67

Argüello-Astorga G, Herrera-Estrella L (1998) Evolution of light-regulated plant promoters. Annu Rev Plant Physiol Plant Mol Biol **49:** 525–555

Armbruster U, Carrillo LR, Venema K, Pavlovic L, Schmidtmann E, Kornfeld A, Jahns P, Berry JA, Kramer DM, Jonikas MC (2014) Ion antiport accelerates photosynthetic acclimation in fluctuating light environments. Nat Commun **5:** 5439

Armbruster U, Leonelli L, Correa Galvis V, Strand D, Quinn EH, Jonikas MC, Niyogi KK (2016) Regulation and levels of the thylakoid K^+/H^+ antiporter KEA3 shape the dynamic response of photosynthesis in fluctuating light. Plant Cell Physiol **57:** 1557–1567

Asada K (1999) The water-water cycle in chloroplasts: Scavenging of active oxygens and dissipation of excess photons. Annu Rev Plant Physiol Plant Mol Biol **50:** 601–639

Athanasiou K, Dyson BC, Webster RE, Johnson GN (2010) Dynamic acclimation of photosynthesis increases plant fitness in changing environments. Plant Physiol **152:** 366–373

Auldridge ME, McCarty DR, Klee HJ (2006) Plant carotenoid cleavage oxygenases and their apocarotenoid products. Curr Opin Plant Biol **9:** 315–321

Baena-González E, Aro EM (2002) Biogenesis, assembly and turnover of photosystem II units. Philos Trans R Soc Lond B Biol Sci **357:** 1451–1459, discussion 1459–1460

Bartoli CG, Yu J, Gómez F, Fernández L, McIntosh L, Foyer CH (2006) Inter-relationships between light and respiration in the control of ascorbic acid synthesis and accumulation in *Arabidopsis thaliana* leaves. J Exp Bot **57:** 1621–1631

Beisel KG, Jahnke S, Hofmann D, Köppchen S, Schurr U, Matsubara S (2010) Continuous turnover of carotenes and chlorophyll *a* in mature leaves of Arabidopsis revealed by $^{14}CO_2$ pulse-chase labeling. Plant Physiol **152:** 2188–2199

Beisel KG, Schurr U, Matsubara S (2011) Altered turnover of β-carotene and Chl *a* in *Arabidopsis* leaves treated with lincomycin or norflurazon. Plant Cell Physiol **52:** 1193–1203

Bellafiore S, Barneche F, Peltier G, Rochaix JD (2005) State transitions and light adaptation require chloroplast thylakoid protein kinase STN7. Nature **433:** 892–895

Bernsdorff F, Döring AC, Gruner K, Schuck S, Bräutigam A, Zeier J (2016) Pipecolic acid orchestrates plant systemic acquired resistance and defense priming via salicylic acid-dependent and -independent pathways. Plant Cell **28:** 102–129

Bieniawska Z, Espinoza C, Schlereth A, Sulpice R, Hincha DK, Hannah MA (2008) Disruption of the Arabidopsis circadian clock is responsible for extensive variation in the cold-responsive transcriptome. Plant Physiol **147:** 263–279

Biswal B (1995) Carotenoid catabolism during leaf senescence and its control by light. J Photochem Photobiol B **30:** 3–13

Bläsing OE, Gibon Y, Günther M, Höhne M, Morcuende R, Osuna D, Thimm O, Usadel B, Scheible WR, Stitt M (2005) Sugars and circadian regulation make major contributions to the global regulation of diurnal gene expression in *Arabidopsis*. Plant Cell **17:** 3257–3281

Bolger AM, Lohse M, Usadel B (2014) Trimmomatic: A flexible trimmer for Illumina sequence data. Bioinformatics **30:** 2114–2120

Bowling SA, Clarke JD, Liu Y, Klessig DF, Dong X (1997) The cpr5 mutant of Arabidopsis expresses both NPR1-dependent and NPR1-independent resistance. Plant Cell **9:** 1573–1584

Brown BA, Jenkins GI (2008) UV-B signaling pathways with different fluence-rate response profiles are distinguished in mature Arabidopsis leaf tissue by requirement for UVR8, HY5, and HYH. Plant Physiol **146:** 576–588

Bruno M, Koschmieder J, Wuest F, Schaub P, Fehling-Kaschek M, Timmer J, Beyer P, Al-Babili S (2016) Enzymatic study on AtCCD4 and AtCCD7 and their potential to form acyclic regulatory metabolites. J Exp Bot **67:** 5993–6005

Caliandro R, Nagel KA, Kastenholz B, Bassi R, Li Z, Niyogi KK, Pogson BJ, Schurr U, Matsubara S (2013) Effects of altered α- and β-branch carotenoid biosynthesis on photoprotection and whole-plant acclimation of *Arabidopsis* to photo-oxidative stress. Plant Cell Environ **36:** 438–453

Casano LM, Martín M, Sabater B (2001) Hydrogen peroxide mediates the induction of chloroplastic Ndh complex under photooxidative stress in barley. Plant Physiol **125:** 1450–1458

Chan KX, Phua SY, Crisp P, McQuinn R, Pogson BJ (2016) Learning the languages of the chloroplast: Retrograde signaling and beyond. Annu Rev Plant Biol **67:** 25–53

Chang CCC, Ślesak I, Jordá L, Sotnikov A, Melzer M, Miszalski Z, Mullineaux PM, Parker JE, Karpińska B, Karpiński S (2009) Arabidopsis chloroplastic glutathione peroxidases play a role in cross talk

between photooxidative stress and immune responses. Plant Physiol **150:** 670–683

Chazdon RL, Pearcy RW (1986) Photosynthetic responses to light variation in rainforest species. II. Carbon gain and photosynthetic efficiency during lightflecks. Oecologia **69:** 524–531

Christ B, Schelbert S, Aubry S, Süssenbacher I, Müller T, Kräutler B, Hörtensteiner S (2012) MES16, a member of the methylesterase protein family, specifically demethylates fluorescent chlorophyll catabolites during chlorophyll breakdown in Arabidopsis. Plant Physiol **158:** 628–641

Christie JM, Suetsugu N, Sullivan S, Wada M (2018) Shining light on the function of NPH3/RPT2-like proteins in phototropin signaling. Plant Physiol **176:** 1015–1024

Covington MF, Maloof JN, Straume M, Kay SA, Harmer SL (2008) Global transcriptome analysis reveals circadian regulation of key pathways in plant growth and development. Genome Biol **9:** R130

Danon A, Coll NS, Apel K (2006) Cryptochrome-1-dependent execution of programmed cell death induced by singlet oxygen in *Arabidopsis thaliana*. Proc Natl Acad Sci USA **103:** 17036–17041

Davison PA, Hunter CN, Horton P (2002) Overexpression of β-carotene hydroxylase enhances stress tolerance in *Arabidopsis*. Nature **418:** 203–206

Demmig-Adams B, Adams WWIII (1992) Carotenoid composition in sun and shade leaves of plants with different life forms. Plant Cell Environ **15:** 411–419

de Souza A, Wang JZ, Dehesh K (2017) Retrograde signals: Integrators of interorganellar communication and orchestrators of plant development. Annu Rev Plant Biol **68:** 85–108

Dłużewska J, Zieliński K, Nowicka B, Szymańska R, Kruk J (2015) New prenyllipid metabolites identified in *Arabidopsis* during photo-oxidative stress. Plant Cell Environ **38:** 2698–2706

Dong MA, Farré EM, Thomashow MF (2011) Circadian clock-associated 1 and late elongated hypocotyl regulate expression of the C-repeat binding factor (CBF) pathway in *Arabidopsis*. Proc Natl Acad Sci USA **108:** 7241–7246

Edwards KD, Anderson PE, Hall A, Salathia NS, Locke JCW, Lynn JR, Straume M, Smith JQ, Millar AJ (2006) *FLOWERING LOCUS C* mediates natural variation in the high-temperature response of the *Arabidopsis* circadian clock. Plant Cell **18:** 639–650

Estavillo GM, Crisp PA, Pornsiriwong W, Wirtz M, Collinge D, Carrie C, Giraud E, Whelan J, David P, Javot H, et al (2011) Evidence for a SAL1-PAP chloroplast retrograde pathway that functions in drought and high light signaling in *Arabidopsis*. Plant Cell **23:** 3992–4012

Evans JR (1987) The relationship between electron transport components and photosynthetic capacity in pea leaves grown at different irradiances. Aust J Plant Physiol **14:** 157–170

Evans JR, Poorter H (2001) Photosynthetic acclimation of plants to growth irradiance: The relative importance of specific leaf area and nitrogen partitioning in maximizing carbon gain. Plant Cell Environ **24:** 755–767

Ezer D, Shepherd SJK, Brestovitsky A, Dickinson P, Cortijo S, Charoensawan V, Box MS, Biswas S, Jaeger KE, Wigge PA (2017) The G-box transcriptional regulatory code in Arabidopsis. Plant Physiol **175:** 628–640

Fahnenstich H, Scarpeci TE, Valle EM, Flügge UI, Maurino VG (2008) Generation of hydrogen peroxide in chloroplasts of Arabidopsis overexpressing glycolate oxidase as an inducible system to study oxidative stress. Plant Physiol **148:** 719–729

Farré EM (2012) The regulation of plant growth by the circadian clock. Plant Biol (Stuttg) **14:** 401–410

Fehér B, Kozma-Bognár L, Kevei E, Hajdu A, Binkert M, Davis SJ, Schäfer E, Ulm R, Nagy F (2011) Functional interaction of the circadian clock and UV RESISTANCE LOCUS 8-controlled UV-B signaling pathways in Arabidopsis thaliana. Plant J **67:** 37–48

Frick G, Su Q, Apel K, Armstrong GA (2003) An *Arabidopsis porB porC* double mutant lacking light-dependent NADPH:protochlorophyllide oxidoreductases B and C is highly chlorophyll-deficient and developmentally arrested. Plant J **35:** 141–153

Gangappa SN, Botto JF (2014) The BBX family of plant transcription factors. Trends Plant Sci **19:** 460–470

Garcion C, Baltensperger R, Fournier T, Pasquier J, Schnetzer MA, Gabriel JP, Métraux JP (2006) FiRe and microarrays: A fast answer to burning questions. Trends Plant Sci **11:** 320–322

Geigenberger P, Thormählen I, Daloso DM, Fernie AR (2017) The unprecedented versatility of the plant thioredoxin system. Trends Plant Sci **22:** 249–262

Gendron JM, Pruneda-Paz JL, Doherty CJ, Gross AM, Kang SE, Kay SA (2012) *Arabidopsis* circadian clock protein, TOC1, is a DNA-binding transcription factor. Proc Natl Acad Sci USA **109:** 3167–3172

Givnish TJ (1988) Adaptation to sun and shade: A whole-plant perspective. Aust J Plant Physiol **15:** 63–92

Grace SC, Logan BA (1996) Acclimation of foliar antioxidant systems to growth irradiance in three broad-leaved evergreen species. Plant Physiol **112:** 1631–1640

Greenham K, McClung CR (2015) Integrating circadian dynamics with physiological processes in plants. Nat Rev Genet **16:** 598–610

Gruner K, Griebel T, Návarová H, Attaran E, Zeier J (2013) Reprogramming of plants during systemic acquired resistance. Front Plant Sci **4:** 252

Hardtke CS, Gohda K, Osterlund MT, Oyama T, Okada K, Deng XW (2000) HY5 stability and activity in *Arabidopsis* is regulated by phosphorylation in its COP1 binding domain. EMBO J **19:** 4997–5006

Harmer SL, Hogenesch JB, Straume M, Chang HS, Han B, Zhu T, Wang X, Kreps JA, Kay SA (2000) Orchestrated transcription of key pathways in *Arabidopsis* by the circadian clock. Science **290:** 2110–2113

Hartmann M, Kim D, Bernsdorff F, Ajami-Rashidi Z, Scholten N, Schreiber S, Zeier T, Schuck S, Reichel-Deland V, Zeier J (2017) Biochemical principles and functional aspects of pipecolic acid biosynthesis in plant immunity. Plant Physiol **174:** 124–153

Havaux M (2014) Carotenoid oxidation products as stress signals in plants. Plant J **79:** 597–606

Hsu PY, Harmer SL (2014) Wheels within wheels: The plant circadian system. Trends Plant Sci **19:** 240–249

Hu H, Rappel WJ, Occhipinti R, Ries A, Böhmer M, You L, Xiao C, Engineer CB, Boron WF, Schroeder JI (2015) Distinct cellular locations of carbonic anhydrases mediate carbon dioxide control of stomatal movements. Plant Physiol **169:** 1168–1178

Huang W, Pérez-García P, Pokhilko A, Millar AJ, Antoshechkin I, Riechmann JL, Mas P (2012) Mapping the core of the Arabidopsis circadian clock defines the network structure of the oscillator. Science **336:** 75–79

Huang W, Hu H, Zhang SB (2015) Photorespiration plays an important role in the regulation of photosynthetic electron flow under fluctuating light in tobacco plants grown under full sunlight. Front Plant Sci **6:** 621

Ischebeck T, Zbierzak AM, Kanwischer M, Dörmann P (2006) A salvage pathway for phytol metabolism in *Arabidopsis*. J Biol Chem **281:** 2470–2477

Jansen M, Gilmer F, Biskup B, Nagel KA, Rascher U, Fischbach A, Briem S, Dreissen G, Tittmann S, Braun S, et al (2009) Simultaneous phenotyping of leaf growth and chlorophyll fluorescence via GROWSCREEN FLUORO allows detection of stress tolerance in *Arabidopsis thaliana* and other rosette plants. Funct Plant Biol **36:** 902–914

Jiao Y, Lau OS, Deng XW (2007) Light-regulated transcriptional networks in higher plants. Nat Rev Genet **8:** 217–230

Johnson GN (2011) Reprint of: Physiology of PSI cyclic electron transport in higher plants. Biochim Biophys Acta **1807:** 906–911

Johnson C, Boden E, Arias J (2003) Salicylic acid and NPR1 induce the recruitment of trans-activating TGA factors to a defense gene promoter in *Arabidopsis*. Plant Cell **15:** 1846–1858

Jones MGK, Outlaw WH, Lowry OH (1977) Enzymic assay of 10^{-7} to 10^{-14} moles of sucrose in plant tissues. Plant Physiol **60:** 379–383

Kaiser E, Matsubara S, Harbinson J, Heuvelink E, Marcelis LFM (2018a) Acclimation of photosynthesis to lightflecks in tomato leaves: Interaction with progressive shading in a growing canopy. Physiol Plant **162:** 506–517

Kaiser E, Morales A, Harbinson J (2018b) Fluctuating light takes crop photosynthesis on a rollercoaster ride. Plant Physiol **176:** 977–989

Karpinski S, Reynolds H, Karpinska B, Wingsle G, Creissen G, Mullineaux P (1999) Systemic signaling and acclimation in response to excess excitation energy in Arabidopsis. Science **284:** 654–657

Kawaguchi R, Girke T, Bray EA, Bailey-Serres J (2004) Differential mRNA translation contributes to gene regulation under non-stress and dehydration stress conditions in *Arabidopsis thaliana*. Plant J **38:** 823–839

Kleine T, Kindgren P, Benedict C, Hendrickson L, Strand A (2007) Genome-wide gene expression analysis reveals a critical role for

CRYPTOCHROME1 in the response of Arabidopsis to high irradiance. Plant Physiol **144:** 1391–1406

Kono M, Terashima I (2016) Elucidation of photoprotective mechanisms of PSI against fluctuating light photoinhibition. Plant Cell Physiol **57:** 1405–1414

Kono M, Noguchi K, Terashima I (2014) Roles of the cyclic electron flow around PSI (CEF-PSI) and O_2-dependent alternative pathways in regulation of the photosynthetic electron flow in short-term fluctuating light in Arabidopsis thaliana. Plant Cell Physiol **55:** 990–1004

Kozuka T, Kong SG, Doi M, Shimazaki K, Nagatani A (2011) Tissue-autonomous promotion of palisade cell development by phototropin 2 in *Arabidopsis*. Plant Cell **23:** 3684–3695

Kromdijk J, Głowacka K, Leonelli L, Gabilly ST, Iwai M, Niyogi KK, Long SP (2016) Improving photosynthesis and crop productivity by accelerating recovery from photoprotection. Science **354:** 857–861

Lai AG, Doherty CJ, Mueller-Roeber B, Kay SA, Schippers JHM, Dijkwel PP (2012) *CIRCADIAN CLOCK-ASSOCIATED 1* regulates ROS homeostasis and oxidative stress responses. Proc Natl Acad Sci USA **109:** 17129–17134

Laisk A, Kiirats O, Oja V (1984) Assimilatory power (postillumination CO_2 uptake) in leaves: Measurement, environmental dependencies, and kinetic properties. Plant Physiol **76:** 723–729

Lätari K, Wüst F, Hübner M, Schaub P, Beisel KG, Matsubara S, Beyer P, Welsch R (2015) Tissue-specific apocarotenoid glycosylation contributes to carotenoid homeostasis in Arabidopsis leaves. Plant Physiol **168:** 1550–1562

Leakey ADB, Press MC, Scholes JD, Watling JR (2002) Relative enhancement of photosynthesis and growth at elevated CO_2 is greater under sunflecks than uniform irradiance in a tropical rain forest tree seedling. Plant Cell Environ **25:** 1701–1714

Leakey ADB, Press MC, Scholes JD (2003) Patterns of dynamic irradiance affect the photosynthetic capacity and growth of dipterocarp tree seedlings. Oecologia **135:** 184–193

Lee HJ, Mochizuki N, Masuda T, Buckhout TJ (2012) Disrupting the bimolecular binding of the haem-binding protein 5 (AtHBP5) to haem oxygenase 1 (HY1) leads to oxidative stress in Arabidopsis. J Exp Bot **63:** 5967–5978

Lee J, He K, Stolc V, Lee H, Figueroa P, Gao Y, Tongprasit W, Zhao H, Lee I, Deng XW (2007) Analysis of transcription factor HY5 genomic binding sites revealed its hierarchical role in light regulation of development. Plant Cell **19:** 731–749

Lefebvre S, Lawson T, Zakhleniuk OV, Lloyd JC, Raines CA, Fryer M (2005) Increased sedoheptulose-1,7-bisphosphatase activity in transgenic tobacco plants stimulates photosynthesis and growth from an early stage in development. Plant Physiol **138:** 451–460

Lemos M, Xiao Y, Bjornson M, Wang JZ, Hicks D, de Souza A, Wang CQ, Yang P, Ma S, Dinesh-Kumar S, et al (2016) The plastidial retrograde signal methyl erythritol cyclopyrophosphate is a regulator of salicylic acid and jasmonic acid crosstalk. J Exp Bot **67:** 1557–1566

Li XP, Björkman O, Shih C, Grossman AR, Rosenquist M, Jansson S, Niyogi KK (2000) A pigment-binding protein essential for regulation of photosynthetic light harvesting. Nature **403:** 391–395

Li XP, Müller-Moulé P, Gilmore AM, Niyogi KK (2002) PsbS-dependent enhancement of feedback de-excitation protects photosystem II from photoinhibition. Proc Natl Acad Sci USA **99:** 15222–15227

Lichtenthaler HK (2007) Biosynthesis, accumulation and emission of carotenoids, α-tocopherol, plastoquinone, and isoprene in leaves under high photosynthetic irradiance. Photosynth Res **92:** 163–179

Lippold F, vom Dorp K, Abraham M, Hölzl G, Wewer V, Yilmaz JL, Lager I, Montandon C, Besagni C, Kessler F, et al (2012) Fatty acid phytyl ester synthesis in chloroplasts of *Arabidopsis*. Plant Cell **24:** 2001–2014

Lisec J, Schauer N, Kopka J, Willmitzer L, Fernie AR (2006) Gas chromatography mass spectrometry-based metabolite profiling in plants. Nat Protoc **1:** 387–396

Liu T, Carlsson J, Takeuchi T, Newton L, Farré EM (2013) Direct regulation of abiotic responses by the Arabidopsis circadian clock component PRR7. Plant J **76:** 101–114

Liu TL, Newton L, Liu MJ, Shiu SH, Farré EM (2016) A G-box-like motif is necessary for transcriptional regulation by circadian pseudo-response regulators in Arabidopsis. Plant Physiol **170:** 528–539

Liu Z, Yan H, Wang K, Kuang T, Zhang J, Gui L, An X, Chang W (2004) Crystal structure of spinach major light-harvesting complex at 2.72 A resolution. Nature **428:** 287–292

Livingston AK, Cruz JA, Kohzuma K, Dhingra A, Kramer DM (2010) An *Arabidopsis* mutant with high cyclic electron flow around photosystem I (hcef) involving the NADPH dehydrogenase complex. Plant Cell **22:** 221–233

Logan BA, Barker DH, Adams WW III, Demmig-Adams B (1997) The response of xanthophyll cycle-dependent energy dissipation in *Alocacia brisbanensis* to sunflecks in a subtropical rainforest. Aust J Plant Physiol **24:** 27–33

Lv F, Zhou J, Zeng L, Xing D (2015) β-Cyclocitral upregulates salicylic acid signalling to enhance excess light acclimation in Arabidopsis. J Exp Bot **66:** 4719–4732

Martín M, Casano LM, Sabater B (1996) Identification of the product of *ndh*A gene as a thylakoid protein synthesized in response to photooxidative treatment. Plant Cell Physiol **37:** 293–298

Martínez IM, Chrispeels MJ (2003) Genomic analysis of the unfolded protein response in Arabidopsis shows its connection to important cellular processes. Plant Cell **15:** 561–576

Martinis J, Glauser G, Valimareanu S, Stettler M, Zeeman SC, Yamamoto H, Shikanai T, Kessler F (2014) ABC1K1/PGR6 kinase: A regulatory link between photosynthetic activity and chloroplast metabolism. Plant J **77:** 269–283

Masuda T, Fusada N, Oosawa N, Takamatsu K, Yamamoto YY, Ohto M, Nakamura K, Goto K, Shibata D, Shirano Y, et al (2003) Functional analysis of isoforms of NADPH:protochlorophyllide oxidoreductase (POR), PORB and PORC, in *Arabidopsis thaliana*. Plant Cell Physiol **44:** 963–974

Matsubara S, Naumann M, Martin R, Nichol C, Rascher U, Morosinotto T, Bassi R, Osmond B (2005) Slowly reversible de-epoxidation of lutein-epoxide in deep shade leaves of a tropical tree legume may 'lock-in' lutein-based photoprotection during acclimation to strong light. J Exp Bot **56:** 461–468

Matsubara S, Krause GH, Aranda J, Virgo A, Beisel KG, Jahns P, Winter K (2009) Sun-shade patterns of leaf carotenoid composition in 86 species of neotropical forest plants. Funct Plant Biol **36:** 20–36

Matsubara S, Schneider T, Maurino VG (2016) Dissecting long-term adjustments of photoprotective and photo-oxidative stress acclimation occurring in dynamic light environments. Front Plant Sci **7:** 1690

Mazor Y, Borovikova A, Caspy I, Nelson N (2017) Structure of the plant photosystem I supercomplex at 2.6 Å resolution. Nat Plants **3:** 17014

McCarthy DJ, Chen Y, Smyth GK (2012) Differential expression analysis of multifactor RNA-Seq experiments with respect to biological variation. Nucleic Acids Res **40:** 4288–4297

Mi H, Muruganujan A, Casagrande JT, Thomas PD (2013) Large-scale gene function analysis with the PANTHER classification system. Nat Protoc **8:** 1551–1566

Michael TP, Breton G, Hazen SP, Priest H, Mockler TC, Kay SA, Chory J (2008a) A morning-specific phytohormone gene expression program underlying rhythmic plant growth. PLoS Biol **6:** e225

Michael TP, Mockler TC, Breton G, McEntee C, Byer A, Trout JD, Hazen SP, Shen R, Priest HD, Sullivan CM, et al (2008b) Network discovery pipeline elucidates conserved time-of-day-specific cis-regulatory modules. PLoS Genet **4:** e14

Mishina TE, Zeier J (2006) The Arabidopsis flavin-dependent monooxygenase FMO1 is an essential component of biologically induced systemic acquired resistance. Plant Physiol **141:** 1666–1675

Mochizuki N, Brusslan JA, Larkin R, Nagatani A, Chory J (2001) *Arabidopsis genomes uncoupled 5* (*GUN5*) mutant reveals the involvement of Mg-chelatase H subunit in plastid-to-nucleus signal transduction. Proc Natl Acad Sci USA **98:** 2053–2058

Mockler TC, Michael TP, Priest HD, Shen R, Sullivan CM, Givan SA, McEntee C, Kay SA, Chory J (2007) The DIURNAL project: DIURNAL and circadian expression profiling, model-based pattern matching, and promoter analysis. Cold Spring Harb Symp Quant Biol **72:** 353–363

Mou Z, Fan W, Dong X (2003) Inducers of plant systemic acquired resistance regulate NPR1 function through redox changes. Cell **113:** 935–944

Munekage Y, Hojo M, Meurer J, Endo T, Tasaka M, Shikanai T (2002) PGR5 is involved in cyclic electron flow around photosystem I and is essential for photoprotection in *Arabidopsis*. Cell **110:** 361–371

Nagel DH, Doherty CJ, Pruneda-Paz JL, Schmitz RJ, Ecker JR, Kay SA (2015) Genome-wide identification of CCA1 targets uncovers an expanded clock network in Arabidopsis. Proc Natl Acad Sci USA **112:** E4802–E4810

Nakamichi N, Kiba T, Kamioka M, Suzuki T, Yamashino T, Higashiyama T, Sakakibara H, Mizuno T (2012) Transcriptional repressor PRR5 directly regulates clock-output pathways. Proc Natl Acad Sci USA **109:** 17123–17128

Návarová H, Bernsdorff F, Döring AC, Zeier J (2012) Pipecolic acid, an endogenous mediator of defense amplification and priming, is a critical regulator of inducible plant immunity. Plant Cell **24:** 5123–5141

Niyogi KK, Grossman AR, Björkman O (1998) Arabidopsis mutants define a central role for the xanthophyll cycle in the regulation of photosynthetic energy conversion. Plant Cell **10:** 1121–1134

Noctor G, Arisi ACM, Jouanin L, Foyer CH (1999) Photorespiratory glycine enhances glutathione accumulation in both the chloroplastic and cytosolic compartments. J Exp Bot **50:** 1157–1167

Noordally ZB, Ishii K, Atkins KA, Wetherill SJ, Kusakina J, Walton EJ, Kato M, Azuma M, Tanaka K, Hanaoka M, et al (2013) Circadian control of chloroplast transcription by a nuclear-encoded timing signal. Science **339:** 1316–1319

Nováková M, Motyka V, Dobrev PI, Malbeck J, Gaudinová A, Vanková R (2005) Diurnal variation of cytokinin, auxin and abscisic acid levels in tobacco leaves. J Exp Bot **56:** 2877–2883

Nozue K, Covington MF, Duek PD, Lorrain S, Fankhauser C, Harmer SL, Maloof JN (2007) Rhythmic growth explained by coincidence between internal and external cues. Nature **448:** 358–361

Oelze ML, Muthuramalingam M, Vogel MO, Dietz KJ (2014) The link between transcript regulation and de novo protein synthesis in the retrograde high light acclimation response of *Arabidopsis thaliana*. BMC Genomics **15:** 320

Oh DH, Kwon CS, Sano H, Chung WI, Koizumi N (2003) Conservation between animals and plants of the cis-acting element involved in the unfolded protein response. Biochem Biophys Res Commun **301:** 225–230

Onda Y, Yagi Y, Saito Y, Takenaka N, Toyoshima Y (2008) Light induction of *Arabidopsis SIG1* and *SIG5* transcripts in mature leaves: Differential roles of cryptochrome 1 and cryptochrome 2 and dual function of SIG5 in the recognition of plastid promoters. Plant J **55:** 968–978

Osmond CB, Grace SC (1995) Perspectives on photoinhibition and photorespiration in the field: Quintessential inefficiencies of the light and dark reactions of photosynthesis? J Exp Bot **46:** 1351–1362

Pal SK, Liput M, Piques M, Ishihara H, Obata T, Martins MCM, Sulpice R, van Dongen JT, Fernie AR, Yadav UP, et al (2013) Diurnal changes of polysome loading track sucrose content in the rosette of wild-type Arabidopsis and the starchless *pgm* mutant. Plant Physiol **162:** 1246–1265

Pearcy RW (1990) Sunflecks and photosynthesis in plant canopies. Annu Rev Plant Physiol Plant Mol Biol **41:** 421–453

Poorter H, Niklas KJ, Reich PB, Oleksyn J, Poot P, Mommer L (2012) Biomass allocation to leaves, stems and roots: Meta-analyses of interspecific variation and environmental control. New Phytol **193:** 30–50

Ramel F, Birtic S, Ginies C, Soubigou-Taconnat L, Triantaphylidès C, Havaux M (2012) Carotenoid oxidation products are stress signals that mediate gene responses to singlet oxygen in plants. Proc Natl Acad Sci USA **109:** 5535–5540

Robinson MD, McCarthy DJ, Smyth GK (2010) edgeR: A Bioconductor package for differential expression analysis of digital gene expression data. Bioinformatics **26:** 139–140

Román Á, Hernández ML, Soria-García Á, López-Gomollón S, Lagunas B, Picorel R, Martínez-Rivas JM, Alfonso M (2015) Non-redundant contribution of the plastidial FAD8 ω-3 desaturase to glycerolipid unsaturation at different temperatures in *Arabidopsis*. Mol Plant **8:** 1599–1611

Rottet S, Devillers J, Glauser G, Douet V, Besagni C, Kessler F (2016) Identification of plastoglobules as a site of carotenoid cleavage. Front Plant Sci **7:** 1855

Ruckle ME, DeMarco SM, Larkin RM (2007) Plastid signals remodel light signaling networks and are essential for efficient chloroplast biogenesis in *Arabidopsis*. Plant Cell **19:** 3944–3960

Ruiz-Sola MÁ, Coman D, Beck G, Barja MV, Colinas M, Graf A, Welsch R, Rütimann P, Bühlmann P, Bigler L, et al (2016) *Arabidopsis* GERANYLGERANYL DIPHOSPHATE SYNTHASE 11 is a hub isozyme required for the production of most photosynthesis-related isoprenoids. New Phytol **209:** 252–264

Schimkat D, Heineke D, Heldt HW (1990) Regulation of sedoheptulose-1,7-bisphosphatase by sedoheptulose-7-phosphate and glycerate, and of fructose-1,6-bisphosphatase by glycerate in spinach chloroplasts. Planta **181:** 97–103

Schmidt H, Kurtzer R, Eisenreich W, Schwab W (2006) The carotenase AtCCD1 from *Arabidopsis thaliana* is a dioxygenase. J Biol Chem **281:** 9845–9851

Schmieder R, Edwards R (2011) Quality control and preprocessing of metagenomic datasets. Bioinformatics **27:** 863–864

Schürmann P, Buchanan BB (2008) The ferredoxin/thioredoxin system of oxygenic photosynthesis. Antioxid Redox Signal **10:** 1235–1274

Sharkey TD, Bernacchi CJ, Farquhar GD, Singsaas EL (2007) Fitting photosynthetic carbon dioxide response curves for C_3 leaves. Plant Cell Environ **30:** 1035–1040

Shen Q, Ho THD (1995) Functional dissection of an abscisic acid (ABA)-inducible gene reveals two independent ABA-responsive complexes each containing a G-box and a novel *cis*-acting element. Plant Cell **7:** 295–307

Simkin AJ, McAusland L, Headland LR, Lawson T, Raines CA (2015) Multigene manipulation of photosynthetic carbon assimilation increases CO_2 fixation and biomass yield in tobacco. J Exp Bot **66:** 4075–4090

Simkin AJ, Lopez-Calcagno PE, Davey PA, Headland LR, Lawson T, Timm S, Bauwe H, Raines CA (2017) Simultaneous stimulation of sedoheptulose 1,7-bisphosphatase, fructose 1,6-bisphophate aldolase and the photorespiratory glycine decarboxylase-H protein increases CO_2 assimilation, vegetative biomass and seed yield in Arabidopsis. Plant Biotechnol J **15:** 805–816

Slattery RA, Walker BJ, Weber APM, Ort DR (2018) The impacts of fluctuating light on crop performance. Plant Physiol **176:** 990–1003

Smith SM, Fulton DC, Chia T, Thorneycroft D, Chapple A, Dunstan H, Hylton C, Zeeman SC, Smith AM (2004) Diurnal changes in the transcriptome encoding enzymes of starch metabolism provide evidence for both transcriptional and posttranscriptional regulation of starch metabolism in Arabidopsis leaves. Plant Physiol **136:** 2687–2699

Stals H, Inzé D (2001) When plant cells decide to divide. Trends Plant Sci **6:** 359–364

Strand DD, Livingston AK, Satoh-Cruz M, Froehlich JE, Maurino VG, Kramer DM (2015) Activation of cyclic electron flow by hydrogen peroxide *in vivo*. Proc Natl Acad Sci USA **112:** 5539–5544

Strand DD, Fisher N, Davis GA, Kramer DM (2016) Redox regulation of the antimycin A sensitive pathway of cyclic electron flow around photosystem I in higher plant thylakoids. Biochim Biophys Acta **1857:** 1–6

Suorsa M, Järvi S, Grieco M, Nurmi M, Pietrzykowska M, Rantala M, Kangasjärvi S, Paakkarinen V, Tikkanen M, Jansson S, et al (2012) PROTON GRADIENT REGULATION5 is essential for proper acclimation of *Arabidopsis* photosystem I to naturally and artificially fluctuating light conditions. Plant Cell **24:** 2934–2948

Suorsa M, Rossi F, Tadini L, Labs M, Colombo M, Jahns P, Kater MM, Leister D, Finazzi G, Aro EM, et al (2016) PGR5-PGRL1-dependent cyclic electron transport modulates linear electron transport rate in *Arabidopsis thaliana*. Mol Plant **9:** 271–288

Takahashi S, Bauwe H, Badger M (2007) Impairment of the photorespiratory pathway accelerates photoinhibition of photosystem II by suppression of repair but not acceleration of damage processes in Arabidopsis. Plant Physiol **144:** 487–494

Takeuchi T, Newton L, Burkhardt A, Mason S, Farré EM (2014) Light and the circadian clock mediate time-specific changes in sensitivity to UV-B stress under light/dark cycles. J Exp Bot **65:** 6003–6012

Terashima I, Hanba YT, Tazoe Y, Vyas P, Yano S (2006) Irradiance and phenotype: Comparative eco-development of sun and shade leaves in relation to photosynthetic CO_2 diffusion. J Exp Bot **57:** 343–354

Thimm O, Bläsing O, Gibon Y, Nagel A, Meyer S, Krüger P, Selbig J, Müller LA, Rhee SY, Stitt M (2004) MAPMAN: A user-driven tool to display genomics data sets onto diagrams of metabolic pathways and other biological processes. Plant J **37:** 914–939

Timm S, Florian A, Fernie AR, Bauwe H (2016) The regulatory interplay between photorespiration and photosynthesis. J Exp Bot **67:** 2923–2929

Tinoco-Ojanguren C, Pearcy RW (1992) Dynamic stomatal behavior and its role in carbon gain during lightflecks of a gap phase and an understory *Piper* species acclimated to high and low light. Oecologia **92:** 222–228

Trimarchi JM, Lees JA (2002) Sibling rivalry in the E2F family. Nat Rev Mol Cell Biol **3:** 11–20

Uematsu K, Suzuki N, Iwamae T, Inui M, Yukawa H (2012) Increased fructose 1,6-bisphosphate aldolase in plastids enhances growth and photosynthesis of tobacco plants. J Exp Bot **63:** 3001–3009

Ulmasov T, Liu ZB, Hagen G, Guilfoyle TJ (1995) Composite structure of auxin response elements. Plant Cell **7:** 1611–1623

Umena Y, Kawakami K, Shen JR, Kamiya N (2011) Crystal structure of oxygen-evolving photosystem II at a resolution of 1.9 Å. Nature **473:** 55–60

Valentin HE, Lincoln K, Moshiri F, Jensen PK, Qi Q, Venkatesh TV, Karunanandaa B, Baszis SR, Norris SR, Savidge B, et al (2006) The *Arabidopsis vitamin E pathway gene5-1* mutant reveals a critical role for phytol kinase in seed tocopherol biosynthesis. Plant Cell **18:** 212–224

Vandepoele K, Quimbaya M, Casneuf T, De Veylder L, Van de Peer Y (2009) Unraveling transcriptional control in Arabidopsis using *cis*-regulatory elements and coexpression networks. Plant Physiol **150:** 535–546

Vialet-Chabrand S, Matthews JSA, Simkin AJ, Raines CA, Lawson T (2017) Importance of fluctuations in light on plant photosynthetic acclimation. Plant Physiol **173:** 2163–2179

Vogel JT, Tan BC, McCarty DR, Klee HJ (2008) The carotenoid cleavage dioxygenase 1 enzyme has broad substrate specificity, cleaving multiple carotenoids at two different bond positions. J Biol Chem **283:** 11364–11373

vom Dorp K, Hölzl G, Plohmann C, Eisenhut M, Abraham M, Weber APM, Hanson AD, Dörmann P (2015) Remobilization of phytol from chlorophyll degradation is essential for tocopherol synthesis and growth of *Arabidopsis*. Plant Cell **27:** 2846–2859

Walley J, Xiao Y, Wang JZ, Baidoo EE, Keasling JD, Shen Z, Briggs SP, Dehesh K (2015) Plastid-produced interorgannellar stress signal MEcPP potentiates induction of the unfolded protein response in endoplasmic reticulum. Proc Natl Acad Sci USA **112:** 6212–6217

Wang W, Barnaby JY, Tada Y, Li H, Tör M, Caldelari D, Lee DU, Fu XD, Dong X (2011) Timing of plant immune responses by a central circadian regulator. Nature **470:** 110–114

Wang X, Wang Q, Han YJ, Liu Q, Gu L, Yang Z, Su J, Liu B, Zuo Z, He W, et al (2017) A CRY-BIC negative-feedback circuitry regulating blue light sensitivity of Arabidopsis. Plant J **92:** 426–436

Watling JR, Ball MC, Woodrow IE (1997a) The utilization of lightflecks for growth in four Australian rain-forest species. Funct Ecol **11:** 231–239

Watling JR, Robinson SA, Woodrow IE, Osmond CB (1997b) Responses of rainforest understorey plants to excess light during sunflecks. Aust J Plant Physiol **24:** 17–25

Wingler A, Lea PJ, Quick WP, Leegood RC (2000) Photorespiration: Metabolic pathways and their role in stress protection. Philos Trans R Soc Lond B Biol Sci **355:** 1517–1529

Xiao Y, Savchenko T, Baidoo EEK, Chehab WE, Hayden DM, Tolstikov V, Corwin JA, Kliebenstein DJ, Keasling JD, Dehesh K (2012) Retrograde signaling by the plastidial metabolite MEcPP regulates expression of nuclear stress-response genes. Cell **149:** 1525–1535

Yadav V, Kundu S, Chattopadhyay D, Negi P, Wei N, Deng XW, Chattopadhyay S (2002) Light regulated modulation of Z-box containing promoters by photoreceptors and downstream regulatory components, COP1 and HY5, in *Arabidopsis*. Plant J **31:** 741–753

Yamori W, Shikanai T (2016) Physiological functions of cyclic electron transport around photosystem I in sustaining photosynthesis and plant growth. Annu Rev Plant Biol **67:** 81–106

Yamori W, Masumoto C, Fukayama H, Makino A (2012) Rubisco activase is a key regulator of non-steady-state photosynthesis at any leaf temperature and, to a lesser extent, of steady-state photosynthesis at high temperature. Plant J **71:** 871–880

Yin ZH, Johnson GN (2000) Photosynthetic acclimation of higher plants to growth in fluctuating light environments. Photosynth Res **63:** 97–107

Zaffagnini M, Bedhomme M, Marchand CH, Morisse S, Trost P, Lemaire SD (2012) Redox regulation in photosynthetic organisms: Focus on glutathionylation. Antioxid Redox Signal **16:** 567–586

Zhang Y, Tessaro MJ, Lassner M, Li X (2003) Knockout analysis of *Arabidopsis* transcription factors TGA2, TGA5, and TGA6 reveals their redundant and essential roles in systemic acquired resistance. Plant Cell **15:** 2647–2653

Zhu XG, Ort DR, Whitmarsh J, Long SP (2004) The slow reversibility of photosystem II thermal energy dissipation on transfer from high to low light may cause large losses in carbon gain by crop canopies: A theoretical analysis. J Exp Bot **55:** 1167–1175